Journal of Medicinal Chemistry

Article

pubs.acs.org/jmc

Identification of Highly Efficacious Glucocorticoid Receptor Agonists with a Potential for Reduced Clinical Bone Side Effects

Christian Harcken,* Doris Riether, Daniel Kuzmich, Pingrong Liu, Raj Betageri, Mark Ralph, Michel Emmanuel, Jonathan T. Reeves, Angela Berry, Donald Souza, Richard M. Nelson, Alison Kukulka, Tazmeen N. Fadra, Ljiljana Zuvela-Jelaska, Roger Dinallo, Jörg Bentzien, Gerald H. Nabozny, and David S. Thomson

Department of Medicinal Chemistry, Department of Immunology and Inflammation, Department of Chemical Development, Boehringer Ingelheim Pharmaceuticals, Inc., 900 Ridgebury Road, Ridgefield, Connecticut 06877, United States

ABSTRACT: Synthesis and structure–activity relationship (SAR) of a series of nonsteroidal glucocorticoid receptor (GR) agonists are described. These compounds contain "diazaindole" moieties and display different transcriptional regulatory profiles in vitro and are considered "dissociated" between gene transrepression and transactivation. The lead optimization effort described in this article focused in particular on limiting the transactivation of genes which result in bone side effects and these were assessed in vitro in MG-63 osteosarcoma cells, leading to the identification of (*R*)-**18** and (*R*)-**21**. These compounds maintained anti-inflammatory activity in vivo in collagen induced arthritis studies in mouse but had reduced effects on bone relevant parameters compared to the widely used synthetic glucocorticoid prednisolone **2** in vivo. To our knowledge, we are the first to report on selective glucocorticoid ligands with reduced bone loss in a preclinical in vivo model.

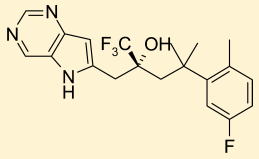

INTRODUCTION

Glucocorticoids (GCs) such as dexamethasone (**1**) and prednisolone (**2**) are being extensively used to treat inflammatory diseases (Figure 1).[1] However, the dose selection and duration of treatment of these drugs is limited by their side effects such as weight gain, hypertension, muscle weakness, skin thinning, diabetes, and GC-induced osteoporosis.[2] For diseases such as rheumatoid arthritis (RA), perhaps the most troublesome and dose-limiting side effect upon chronic treatment with low dose GCs is GC-induced osteoporosis, leading to a weakening of trabecular bone and a significant increase in the risk of spine, hip, and rib fractures.[3]

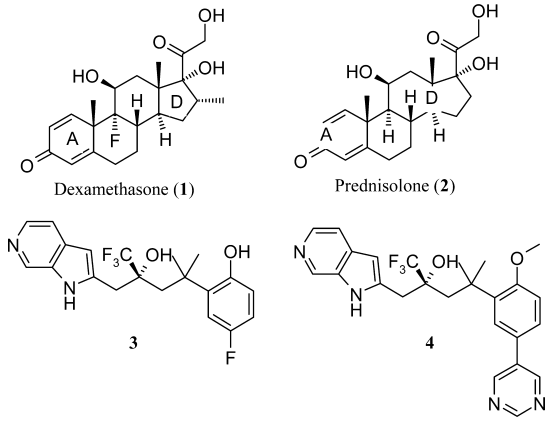

Figure 1. Synthetic glucocorticoid agonists.

Glucocorticoids exert their pharmacological effect through interaction with the glucocorticoid receptor (GR), a member of the nuclear receptor super family. When the GR binds an agonist ligand in the cytosol, it sheds chaperone proteins and translocates to the nucleus.[4] Here the receptor–ligand complex regulates transcription either positively or negatively.[5] The precise molecular mechanism of GC-mediated effects are highly complex and only partially understood.[6] Since the early 2000s, a possibly oversimplistic hypothesis has been widely accepted among researchers aiming at safer alternatives to classical GCs. This hypothesis describes two distinct pathways of the receptor–ligand complex: (1) As a homodimer the receptor–ligand complex acts itself as transcription factor by interacting directly with Glucocorticoid response elements (GRE) on the DNA, upregulating transcription of respective genes. This pathway has been called transactivation (TA) and has been attributed to many of the GC mediated side effects. (2) The receptor–ligand complex indirectly affects transcription, interacting in a monomeric form with transcription factors such as NF-κB and AP-1, downregulating the transcription of genes.[7] This pathway has, in a broader sense, been called transrepression (TR) and is considered primarily responsible for the anti-inflammatory effects of GCs as it results in down-regulation of key cytokine inflammatory mediators such as TNF-α, IL-1, IL-2, and IL-6. This hypothesis of the two distinct pathways owes its genesis to a series of experiments described elsewhere and has been the basis of "dissociated" GCs.[8] Evidence has continued to accumulate to support the existence of transrepression as a means of downregulating pro-inflammatory cells.[9] However, data generated more recently do not support and partially even contradict the hypothesis and

Received: December 13, 2013
Published: February 7, 2014

Scheme 1. General Synthesis of Diazaindoles

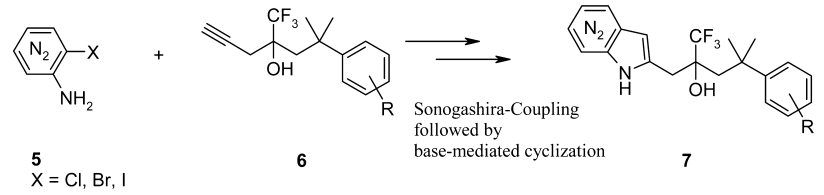

5
X = Cl, Br, I

6

7

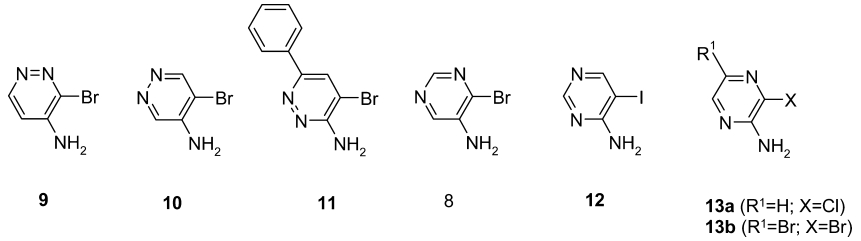

9 10 11 8 12

13a (R^1=H; X=Cl)
13b (R^1=Br; X=Br)

Figure 2. Halogenated aminoarenes.

Scheme 2. Synthesis of Diazaindole Isomers[a]

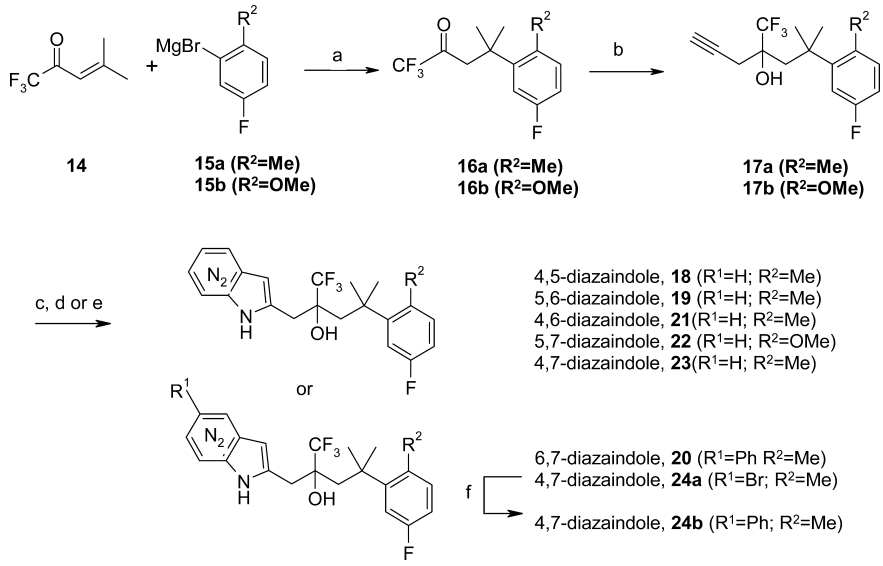

14

15a (R^2=Me)
15b (R^2=OMe)

16a (R^2=Me)
16b (R^2=OMe)

17a (R^2=Me)
17b (R^2=OMe)

4,5-diazaindole, **18** (R^1=H; R^2=Me)
5,6-diazaindole, **19** (R^1=H; R^2=Me)
4,6-diazaindole, **21**(R^1=H; R^2=Me)
5,7-diazaindole, **22** (R^1=H; R^2=OMe)
4,7-diazaindole, **23**(R^1=H; R^2=Me)

6,7-diazaindole, **20** (R^1=Ph R^2=Me)
4,7-diazaindole, **24a** (R^1=Br; R^2=Me)
4,7-diazaindole, **24b** (R^1=Ph; R^2=Me)

[a]Reagents and conditions: (a) arylbromide, Mg (1.2 equiv), THF, reflux, 3 h, then CuI (1.1 equiv), −10 °C, 1 h; then **14** (1.1 equiv), room temperature, 16 h; (b) Al (3 equiv), $HgCl_2$ (0.02 equiv), THF, 0 °C, 10 min, propargylbromide (3 equiv), 50 °C, 1 h, then **16**, −78 °C to room temperature, 2 h, yield 99%; (c) **8**−**13** (1 equiv), $Pd(PPh_3)_2Cl_2$ (0.05 equiv), CuI (0.1 equiv), DMF, NEt_3, room temperature, 15 h, yield 32−75%; (d) NMP, KO*t*Bu (2.2 equiv), room temperature, 17 h, yield 15−36% over 2 steps; (e) pyridine (3 equiv), AcCl (2 equiv), CH_2Cl_2, 0 °C, 1 h; tetramethylguanidine (5 equiv), DMSO, 140 °C, μwave, 10 min, yield 18% over 2 steps; (f) $Pd(PPh_3)_4$ (0.1 equiv), $PhB(OH)_2$ (2 equiv), K_2CO_3 (3 equiv), DMF/MeOH/DME, 80 °C, 3 h, yield 71%.

left it experimentally poorly supported.[6] Nevertheless, for an industrial drug discovery program, the hypothesis has served as a highly appealing working model throughout the past decade[10] that has sparked the search for a functionally selective, so-called "dissociated" synthetic glucocorticoid that could potentially offer a therapeutic advantage over currently marketed GCs.[11]

In addition, many of the clinically used GCs also interact with other nuclear receptors, especially the progesterone receptor (PR) and the mineralocorticoid receptor (MR). Therefore, an improved selectivity over other nuclear receptors is also desirable.

Previously, we have disclosed nonsteroidal GC mimetics,[12−14] including a series of trifluoromethylcarbinol derived compounds.[15−17] Therein we described the identification and profile of azaindole compounds such as **3** and **4** that have demonstrated excellent nuclear receptor selectivity, potent GR binding, potent GR agonism (as indicated by their in vitro suppression of IL-1 induced IL-6 production in human foreskin fibroblasts), and excellent in vivo activity in acute models of inflammation (such as inhibition of LPS induced TNF-α production in mouse) and in chronic disease models (such as inhibition of collagen-induced arthritis in mouse) (Figure 1). In addition, these compounds showed reduced transactivation (as indicated in vitro by their reduced potency and maximum efficacy in an MMTV-promoter transfected HeLa cell and their reduced incidence of metabolic side effects upon chronic dosing in vivo). However, for a bone relevant dissociation marker (such as suppression of vitamin D stimulated osteocalcin production in MG-63 osteosarcoma cells) these compounds did show only a moderately attenuated effect compared to

dx.doi.org/10.1021/jm4019178 | J. Med. Chem. 2014, 57, 1583−1598

Scheme 3. Synthesis of 5-Substituted 4,6-Diazaindoles[a]

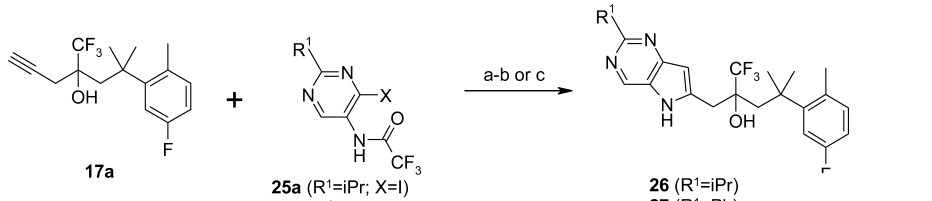

[a]Reagents and conditions: (a) $Pd(PPh_3)_2Cl_2$ (0.05 equiv), CuI (0.1 equiv), DMF, NEt_3, room temperature, 15 h, yield 36−57%; (b) tetramethylguanidine (5 equiv), dioxane, 90 °C, 15 min, yield 33−64%; (c) $Pd(PPh_3)_2Cl_2$ (0.1 equiv), CuI (0.1 equiv), MeCN, NEt_3, 70 °C, 2 h, yield 57−72%.

prednisolone. Encouraged by the results achieved thus far, we next decided to tackle the question whether an even more desirable profile is possible, i.e., achieving dissociation for bone side effect relevant markers.

Previous studies had revealed that the position of the pyridine nitrogen atom in the azaindole moiety of compounds such as **3** was of utmost importance.[16] Whereas the 4-, 5-, 6-, and 7-azaindole are all potent GR ligands, they showed anti-inflammatory potency to a different degree: the 5- and 6-azaindole were potent agonists, whereas the 4- and 7-azaindole displayed almost no anti-inflammatory efficacy in vitro.[16] It was speculated that the pyridine nitrogen in the 5- and 6-azaindole can form an H-bonding interaction with GLU570 and ARG611 of the GR, mimicking the interaction of the steroid A-ring. It is conceivable that this may result in a conformational change required to achieve an agonist conformation of the ligand−receptor complex. This publication describes the synthesis and biological evaluation of azaindole derived heteroaryl moieties as A-ring mimetics that contain two nitrogen atoms in the six-membered ring ("diazaindoles") with a particular focus on optimization for bone dissociation.

CHEMISTRY

The general strategy to synthesize the isomers of diazaindoles **7** consists of the Sonogashira coupling of an alkyne **6** with an appropriately halogenated aminoheteroarene **5** and subsequent base catalyzed cyclization (Scheme 1).[18] The desired halogenated heteroarylamines **8**−**13** were prepared the following way (Figure 2): **8**, **9**, **10**, and **12** were prepared by bromination or iodination of the corresponding aminoarenes.[19] **11** was prepared in four steps from acyclic precursors.[20] **13a** was prepared in one step from 2,3-dichloropyrazine.[21] **13b** was commercially available.

The synthesis of alkynes **17** begins with the addition of appropriately substituted arylmagnesium bromide reagents **15** to the trifluoromethylenone **14** (Scheme 2).[16] The resulting ketones **16** are then treated with propargyl aluminum to yield the racemic alkynes **17**. Alternatively, the ketones can be transformed in four steps to the enantiopure (*S*)-isomers of **17**.[22] The alkynes **17** and halogenated aminoarenes **8**−**13** were treated with a Pd catalyst to afford the Sonogashira coupling. The resulting coupling product was then either treated with KO*t*Bu in *N*-methylpyrrolidinone or *N*-acylated and subsequently treated with tetramethylguanidine in dioxane to effect the cyclization to the diazaindole **18**−**23** and **24a** (cyclization procedure A and B, respectively). **24a** was subjected to a Suzuki coupling to give the 5-phenyl-substituted derivative **24b**.

5-Substituted 4,6-diazaindoles **26**−**31** were prepared analogously by Sonogashira coupling of alkyne **17a** with appropriately substituted brominated trifluoroacetylamino pyrimidines **25a**−**f** (Scheme 3). **25a**,[19] **25b**,[19] and **25c** were prepared in six steps from acyclic precursors. **25d** and **25e** were prepared in five steps from acyclic precursors. **25f** was prepared in four steps from 5-chloro-2-nitropyrimidine. The coupling products were cyclized using tetramethylguanidine in dioxane to give the 5-substituted 4,6-diazaindoles **26**−**31**.

4,6-Diazaindoles with additionally substituted right-hand side rings **32**−**35** were prepared from the aminobromopyrimidine **12** and alkynes **17b**−**e** (Scheme 4). Alkynes **17b**,[16] **17d**, and **17e** were prepared in analogy to **17a**. Alkyne **17c** was prepared in eight steps from 4′-fluoro-2′-hydroxy-acetophenone. Diazaindoles **36** and **37** were synthesized from alkynes **17f**−**g**, which were prepared in five and six steps respectively from ethyl trifluoropyruvate[16] (Scheme 5). Diazaindole **40** was prepared through acylation and subsequent cyclization of 5-amino-4-methylpyrimidine **38** with the ester **39** (Scheme 6). Diazaindoles **41** and **42** were prepared by demethylation of the corresponding methoxy analogue **32** and **33** with BBr_3, respectively (Scheme 7).

The pure enantiomers (*R*)-**18** and (*R*)-**21** (>98% *ee*) were synthesized following the same sequence outlined in Scheme 1 using enantiopure alkynes **6**, which have been described elsewhere.[16,22]

Scheme 4. Synthesis of 4,6-Diazaindoles[a]

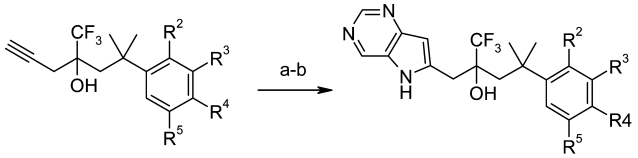

[a]Reagents and conditions: (a) **12** (1 equiv), $Pd(PPh_3)_2Cl_2$ (0.05 equiv), CuI (0.1 equiv), DMF, NEt_3, room temperature, 15 h, yield 53−71%; (b) NMP, KO*t*Bu (2.2 equiv), room temperature, 17 h, yield 25−63%.

dx.doi.org/10.1021/jm4019178 | J. Med. Chem. 2014, 57, 1583−1598

Scheme 5. Synthesis of Dihydrobenzofuran Containing Analogues[a]

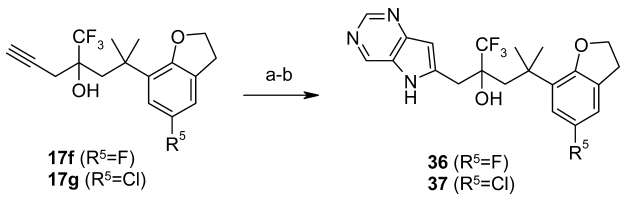

17f (R^5=F)
17g (R^5=Cl)

36 (R^5=F)
37 (R^5=Cl)

[a]Reagents and conditions: (a) **8** (1 equiv), $Pd(PPh_3)_2Cl_2$ (0.05 equiv), CuI (0.1 equiv), DMF, NEt_3, room temperature, 15 h, yield 24−47%; (b) NMP, KO*t*Bu (2.2 equiv), room temperature, 17 h, yield 41−50%.

Scheme 6. Synthesis of Diazaindole 40[a]

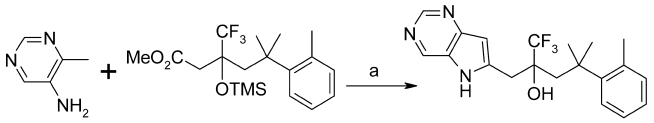

38 **39** **40**

[a]Reagents and conditions: (a) **38** (3.3 equiv), *n*BuLi (8.2 equiv), THF, −20 °C to room temperature, 2.5 h; **39**, THF, room temperature, 20 min, HCl (6 N), 2 h, yield 47%.

Scheme 7. Synthesis of Phenole Containing Analogues[a]

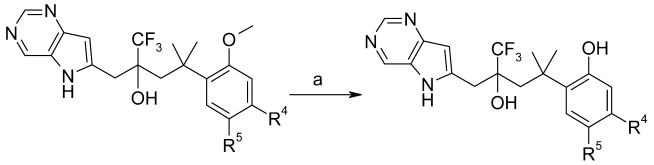

32 (R^4=H; R^5=F)
33 (R^4=F; R^5=H)

41 (R^4=H; R^5=F)
42 (R^4=F; R^5=H)

[a]Reagents and conditions: (a) BBr_3 (1 equiv), DCM, 0 °C, 18−60 h, yield 68−70%.

RESULTS AND DISCUSSION

All possible isomers of the racemic diazaindoles **18**−**23** were synthesized. Because of synthetic accessibility, the 6,7-diazaindole **20** was synthesized bearing an additional 5-phenyl substituent. The 5,7-diazaindole **22** was prepared with a methoxy substituted phenyl ring on the right-hand side of the molecule instead of the methyl substituted phenyl group. These two groups were previously shown to be equivalent in their in vitro biological profile.[16] The prepared diazaindole isomers were all potent GR binders, indicated by their ability to compete for receptor binding with tetramethylrhodamine labeled dexamethasone (Table 1). It was previously hypothesized that the nitrogen atoms of 5-azaindoles and 6-azaindoles interact with the arginine−glutamine pair of the steroid A-ring binding pocket.[16] Diazaindole compounds such as **21** dock the same way into the GR-LBD using the GR-LBD/dexamethasone co-complex X-ray structure[23] (Figure 3).

The 5,6-diazaindole **19** and the 5,7-diazaindole **22** showed potent affinity to the progesterone receptor (PR) and the mineralocorticoid receptor (MR), the MR/GR selectivity for **19** and **22** was merely 28- and 40-fold, respectively. Except for the 5,7-diazaindole **23**, all compounds were shown to be GR agonists, indicated by inhibiting IL-1 stimulated IL-6 production in human foreskin fibroblast (HFF), with a lower maximum efficacy compared to dexamethasone.[24] The SAR to identify partial agonists of varying degree and/or compounds with varying degree of dissociation remained largely empirical. The 5-phenyl-substituted 4,7-diazaindole **24b** showed agonism, albeit with an IC_{50} of 170 nM at a reduced potency. To assess the potential dissociation of these analogues, the selective agonist compounds were counterscreened for their ability to activate the MMTV promoter in HeLa cells transfected with an MMTV luciferase construct. The 6,7-diazaindole **20** showed potent transactivation in this marker, whereas the 4,5- and 4,6-diazaindoles **18** and **21** showed no or minimal activity in this assay. It has been described before in the literature that increased potency can be achieved upon increasing the steric demand of the A-ring mimic above a certain threshold.[25]

To further assess the SAR in this class of compounds, additional racemic analogues were prepared with the 4,6-diazaindole A-ring mimetic. Table 2 shows the effect of substitution in the 5-position of the 4,6-diazaindole.

Substitution at the 5-position did not affect the GR binding potency significantly. The analogues **26**−**31** show excellent nuclear receptor selectivity, with the exception of **30**, that for unknown reasons shows increased MR activity. The isopropyl analogue **26** and the pyrrolidinyl analogue **29** show significantly reduced transrepression potency with IC_{50} values of 560 and 130 nM, respectively. The sterically more demanding phenyl, pyridyl, and 1,1-dioxo-thiomorpholin-4-yl analogues **27**, **28**, and **31** retain their transrepression potency, however, they show increased activity in the MMTV reporter assay with 36%, 32%, and 22% maximum efficacy, respectively, indicating a less dissociated profile. Again, it has been described before in the literature that increased potency can be achieved upon increasing the steric demand of the A-ring mimic above a certain threshold.[25]

Table 3 shows the effect of changes in substitution pattern on the right-hand side phenyl group. Replacement of the methyl group in **21** with a methoxy group in compound **32** or a hydroxy group as in **41** is well tolerated: **32** and **41** retain the nuclear receptor selectivity as well as the agonist potency of **21**. Moving the fluoro substituent from the 5-position to the 4-position as in **42** results in reduced nuclear receptor selectivity. This has been observed before in related series.[16] Complete removal of the fluoro substituent from **21** as in **40** results in a slight loss in potency and maximum efficacy. It has been demonstrated before that complete removal of 2-substitution also results in a dramatic loss of transrepression potency.[16] Docking of compound **21** suggests that the phenyl group resides in a space occupied by the steroid D-ring of dexamethasone. Formal cyclization of an alkoxy group with the 3-position of the right-hand side phenyl ring results in the formation of a dihydrofuran moiety. Dihydrofuran compounds **36** and **37** show a slightly increased affinity to the progesterone receptor, however, they retain potent transrepression activity. The replacement of the hydroxy group with a larger hydrogen bond acceptor group such as the methylsulfonyl group in **34** also maintains selectivity and agonist potency. Moving the sulfonyl group to the 3-position is not tolerated: compound **35** shows significantly reduced binding affinity and no transrepression activity. This is presumed to be due to increased steric clashes in the D-ring binding pocket. Large substituents to access an expanded D-ring pocket can be accessed by 3-aryl substitution on the D-ring mimic as described previously.[16]

To assess the dissociation profile of compounds with regard to potential bone side effects, compounds with the appropriate selectivity and potency profile were tested for suppression of vitamin D induced osteocalcin production in human MG-63

dx.doi.org/10.1021/jm4019178 | J. Med. Chem. 2014, 57, 1583−1598

Table 1. Azaindole Isomers

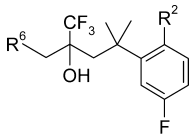

compd no.	R^6	R^2	GR IC_{50} [nM][a]	PR IC_{50} [nM]	MR IC_{50} [nM]	IL-6 IC_{50} [nM] and max. efficacy [%][b]	MMTV max. efficacy at 2 μM [%][b]
18		Me	7	>2000	615	16 (85%)	7%
19		Me	3	490	83	5 (89%)	NT[c]
20	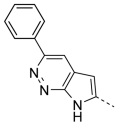	Me	13	>2000	>2000	6 (96%)	75%
21		Me	8	>2000	855	19 (74%)	0%
22		OMe	4	1450	160	10 (82%)	NT
23		Me	57	>2000	>2000	>2000	NT
24b	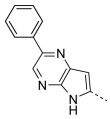	Me	11	>2000	>2000	170 (82%)	NT

[a]IC_{50} values are the mean of at least two values, each determined from duplicate 11-point concentration response curves [b]Maximum efficacy at the highest tested concentration compared to dexamethasone, defined at 100%; maximum concentration tested is 2 μM. [c]NT = not tested.

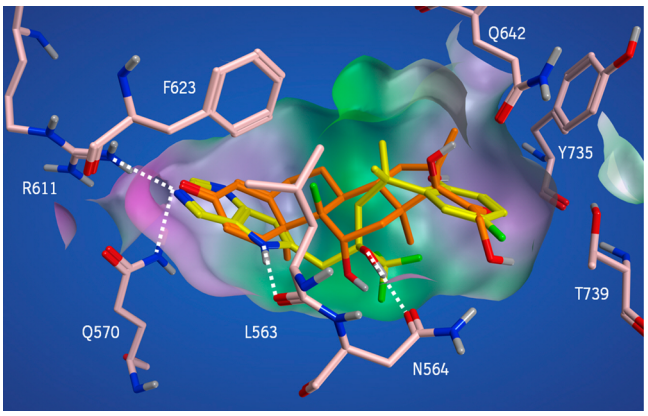

Figure 3. Docking results for (*R*)-**21** (yellow) into the GR-LBD/dexamethasone (orange) co-complex X-ray structure.[23] Potential H-bonds of (*R*)-**21** with the protein are indicated by white lines. Docking was performed using Glide (Small-Molecule Drug Discovery Suite 2013−2: Glide, version 6.0, Schrödinger, LLC, New York). The picture was generated with MOE (Molecular Operating Environment 2012, Chemical Computing Group Inc., Montreal, QC, Canada).

osteosarcoma cells. Table 4 shows the results for selected compounds. All tested compounds showed significantly reduced maximal efficacy for the suppression in osteocalcin production in this assay compared to dexamethasone. However, **3** had not shown statistically significantly reduced GC-mediated bone side effects in a chronic model of mouse collagen-induced arthritis (CIA).[16] Therefore, a maximal efficacy lower than that of **3** in this assay was desirable, assuming osteocalcin is a viable biomarker for bone formation rate related side effects. Compounds **21**, **18**, **42**, **37**, **41**, **36**, and **34** all showed maximal efficacies <50%. Compound **21** and **18**, as potent and NR-selective, and additionally osteocalcin-dissociated analogues were selected for further study.

It should be noted that while these compounds show the desired pharmacology profile and are suitable tools to assess the dissociation in vivo, their drug-like properties are suboptimal. Compounds **21** and **18** show low aqueous crystalline solubility of 11 and 2 μg/mL in buffer at pH 7, respectively. Both compound are predicted to be rapidly metabolized in human with a human liver microsome clearance rate of >89% Qh. Both compounds show good membrane permeability of 11 and 13 × 10^{-6} cm/s in Caco-2 cells, respectively, and no detectable efflux.

The active enantiomers (*R*)-**18** and (*R*)-**21** were selected for profiling in vivo to assess how well the in vitro osteocalcin marker predicts attenuated GC-mediated side effects in vivo (Table 5). It has been demonstrated previously that all activity of the racemic mixtures in this class of GR agonists resides in the (*R*)-enantiomer.[16] As predicted by their in vitro ADME profile, the pharmacokinetic profile of both compounds is

dx.doi.org/10.1021/jm4019178 | J. Med. Chem. 2014, 57, 1583−1598

Table 2. 5-Substituted 4,6-Diazaindoles

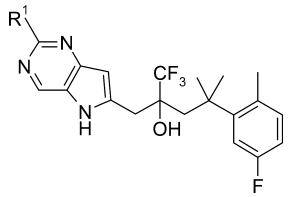

compd no.	R^1	GR IC_{50} [nM][a]	PR IC_{50} [nM]	MR IC_{50} [nM]	IL-6 IC_{50} [nM] and max. efficacy [%][b]	MMTV max. efficacy at 2 μM [%][b]
21	H	8	>2000	855	19 (74%)	0%
26	iPr	26	>2000	>2000	560 (50%)	NT[c]
27	Ph	5	>2000	1900	8 (93%)	36%
28		5	>2000	>2000	12 (92%)	32%
29		18	>2000	>2000	130 (76%)	NT
30		5	1400	170	15 (84%)	NT
31		8	>2000	>2000	19 (84%)	22%

[a]IC_{50} values are the mean of at least two values, each determined from duplicate 11-point concentration response curves. [b]Maximum efficacy at the highest tested concentration compared to dexamethasone, defined at 100%; maximum concentration tested is 2 μM. [c]NT = not tested.

suboptimal: (*R*)-**18** showed high clearance (>100% Qh) and moderate volume of distribution (V_{ss} = 3.7 L/kg), resulting in a short half-life ($t_{1/2}$ = 0.5 h) and correspondingly low bioavailability (9%*F*) in rat PK (2 mg/kg iv in 80/20 PEG/water; 30 mg/kg po in 80/18/2 PEG/water/Tween). (*R*)-**21** also showed high clearance (61% Qh) and moderate volume of distribution (V_{ss} = 2.1 L/kg) resulting in a short half-life ($t_{1/2}$ = 0.6 h) and correspondingly low bioavailability (13%*F*) in rat PK (5 mg/kg iv in 80/20 PEG/water; 30 mg/kg po in 80/18/2 PEG/water/Tween). No PK/PD analysis was performed.

Both compounds showed potent inhibition of LPS-stimulated TNF-α production in mouse in vivo consistent with potent anti-inflammatory transrepression activity (dosed po in 30% cremophor; (*R*)-**21** ED_{50} 1−3 mg/kg; (*R*)-**18** ED_{50} 3−10 mg/kg; data not shown). Furthermore, these compounds were tested in a collagen-induced arthritis model, a chronic model of inflammatory polyarthritis that shares many features with human rheumatoid arthritis. B10.RIII mice were immunized with porcine type II collagen and complete Freund's adjuvant and then monitored for signs of arthritis. Animals were enrolled into the study at the first signs of disease (paw/joint swelling) and treated daily with compound, prednisolone, or vehicle for a period of five weeks. The animals were monitored regularly and arthritis severity was assessed through clinical scoring of all four paws based on a score of 1−4. The clinical score per paw was summed to give a maximal severity score of 16 for each animal. (*R*)-**21** was evaluated in this model at once daily oral doses of 100 mg/kg for a period of five weeks versus prednisolone at 30 and 3 mg/kg. At the end of the study, serum was collected for biomarker analysis to assess the side effect profile. (*R*)-**21** significantly inhibited disease progression (57% inhibition by AUC vs vehicle; Mann−Whitney test: $p < 0.05$) (Figure 4). Plasma concentrations were determined after a single dose of 100 mg/kg in satellite animals (B10.RIII mice, *n* = 3, 4320 nM at c_{max}). Prednisolone reached 43% and 78% disease score reduction at 3 and 30 mg/kg doses, respectively. (*R*)-**18** was tested at 100 mg/kg in a separate experiment and showed 53% reduction in disease score, comparable to prednisolone at 3 mg/kg (53% inhibition in this study). Plasma concentrations were determined after a single dose of 100 mg/kg in satellite animals (B10.RIII mice, *n* = 3, 38900 nM at c_{max}). Prednisolone at 30 mg/kg showed 90% inhibition in this study. The difference in prednisolone response between the two studies is assumed to be caused by differences in the exposure of prednisolone in the utilized vehicles.

Table 6 lists the side-effect markers for (*R*)-**18** and (*R*)-**21**. Both compounds clearly showed reduced effects on metabolic side effect markers such as % body fat, free fatty acids, and insulin. (*R*)-**21** was also tested for the effect on triglycerides. Both test compounds showed statistically significant reduction in free fatty acids compared to the approximately equi-efficacious dose of 3 mg/kg prednisolone. The other metabolic side effect markers did not reach statistical significance comparing the compound treated group to the group treated with prednisolone at 3 mg/kg, however, all of them trended in a favorable direction. This profile had been demonstrated before with **3** and is believed to be predicted by in vitro dissociation for the MMTV marker.[16] To assess the in vivo bone dissociation profile, the study was repeated with nonimmunized mice because the diseased state of the CIA study mice interferes with bone-relevant readouts. Nondiseased, age-matched mice were dosed with (*R*)-**18** or (*R*)-**21** at the same doses and for the same duration as in the prior study of immunized mice. MicroCT analysis for femur cortical thickness demonstrated significantly reduced bone loss over the treatment course. (*R*)-**21** showed only 6% reduction in mean femur cortical thickness at the 100 mg/kg dose (57% CIA disease score reduction) compared to the less efficacious 3 mg/kg dose of prednisolone

dx.doi.org/10.1021/jm4019178 | J. Med. Chem. 2014, 57, 1583−1598

Table 3. 4,6-Diazaindole Analogues

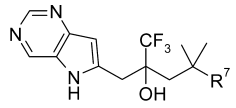

compd no.	R^7	GR IC_{50} [nM][a]	PR IC_{50} [nM]	MR IC_{50} [nM]	IL-6 IC_{50} [nM] and max. efficacy [%][b]	MMTV max. efficacy at 2 μM [%][b]
21		8	>2000	855	19 (74%)	0%
32	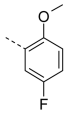	9	>2000	>2000	21 (85%)	5%
41	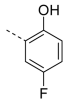	7	>2000	1150	11 (91%)	NT[d]
42		5	880	1200	9 (86%)	22%
40		13	>2000	1100	44 (69%)	NT
36	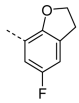	7	1400	1300	24 (78%)	NT
37	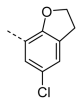	5	1700	340	13 (87%)	12%
34		24	>2000	>2000	21 (92%)	NT
35		840	>2000	>2000	NT	NT

[a]IC_{50} values are the mean of at least two values, each determined from duplicate 11-point concentration response curves. [b]Maximum efficacy at the highest tested concentration compared to dexamethasone, defined at 100%; maximum concentration tested is 2 μM. [c]NT = not tested.

(43% CIA disease score reduction) that caused 9% reduction in mean femur cortical thickness (Table 7). This difference does not reach statistical significance, however, this is not unexpected because the two groups being compared are not equi-efficacious (57% vs 43% reduction in CIA disease score). (*R*)-**18** showed only 8% reduction at the 100 mg/kg dose compared to the equi-efficacious 3 mg/kg dose of prednisolone that caused 13% reduction. This difference reaches statistical significance. This difference was maintained after 10 weeks of treatment (data not shown). The difference in prednisolone response between the two studies is assumed to be caused by differences in the exposure of prednisolone in the utilized vehicles (not measured).

CONCLUSION

The described nonsteroidal trifluoromethylcarbinol scaffold has provided multiple glucocorticoid mimetics with potent GR binding affinity and favorable nuclear receptor selectivity. Compounds from this series have been established as having excellent anti-inflammatory in vivo activity. By optimizing the steroid-A-ring mimetic portion and the right-hand-side substituents of these analogues, compounds with reduced in vitro osteocalcin production suppression were identified. These compounds demonstrated reduced GC-mediated osteoporosis in chronic treatment in mouse in vivo. This constitutes a significant milestone in the development of dissociated GCs. Compounds with a biological profile like **18** and **21** have tremendous potential to show a significant clinical benefit over existing GC treatment options. However, identification of a viable clinical candidate will require further optimization of drug-like properties of these compounds and will be disclosed in due course.

EXPERIMENTAL SECTION

Analytical Methods. ^1H NMR spectra were recorded on a Bruker UltraShield 400 MHz spectrometer operating at 400 MHz in solvents, as noted. Proton coupling constants (*J* values) are rounded to the nearest Hz. All solvents were HPLC grade or better. The reactions were followed by TLC on precoated Uniplate silica gel plates purchased from Analtech. The developed plates were visualized using 254 nm UV illumination or by PMA stain. Flash column

dx.doi.org/10.1021/jm4019178 | J. Med. Chem. 2014, 57, 1583−1598

Table 4. Inhibition of Osteocalcin Production

compd no.	osteocalcin suppression max efficacy at 2 μM [%][a,b]
1 (dex)	100
2 (pred)	78
3	68
4	45
18	45
19	81
20	73
21	32
27	72
28	74
31	80
34	43
36	26
37	35
41	42
42	28

[a]IC_{50} values are the mean of at least two values, each determined from duplicate 11-point concentration response curves. [b]Maximum efficacy at the highest tested concentration compared to dexamethasone, defined at 100%; maximum concentration tested is 2 μM.

Table 5. In Vitro Profile of Active Enantiomers (*R*)-18 and (*R*)-21

compd no.	GR IC_{50} [nM][a]	PR IC_{50} [nM]	MR IC_{50} [nM]	IL-6 IC_{50} [nM] and max. efficacy [%][b]	MMTV max. efficacy at 2 μM [%][b]	Osteocalcin suppression max. efficacy at 2 μM [%][b,c]
(*R*)-**18**	5	>2000	260	9 (86)	0	34
(*R*)-**21**	4	>2000	475	13 (72)	0	32

[a]IC_{50} values are the mean of at least two values, each determined from duplicate 11-point concentration response curves. [b]Maximum concentration tested is 2 μM. [c]Maximum efficacy at the highest tested concentration compared to dexamethasone, defined at 100%.

chromatography on silica gel was performed on Redi Sep prepacked disposable silica gel columns using an Isco Combiflash or on traditional gravity columns. Reactions were carried out under an atmosphere of argon. Purity was evaluated by analytical HPLC using a Varian Dynamax SD-200 pump coupled to a Varian Dynamax UV-1 detector: (A) water + 0.05% TFA and (B) acetonitrile + 0.05% TFA, flow 1.2 mL/min. Column Vydac RP-18, 5 m, 250 mm × 4.6 mm, photodiode array detector at 220 or 254 nm; from 95% to 20% solvent (A) over 20 min. All compounds were 95% or greater purity by HPLC with the exception of **22** (no HPLC data), **37** (94%), and **42** (92%).

Chemistry Experimental. *General Sonogashira Coupling Procedure.* To a solution of halogeno diazine **8**–**13** (1 mmol) in anhydrous DMF (1 mL) and NEt_3 (3 mL) wais added CuI (0.10 mmol), $Pd(PPh_3)_2Cl_2$ (0.05 mmol) and the alkyne **17** (1 mmol) under argon and the reaction stirred at room temperature for 15 h. The reaction was diluted with EtOAc (10 mL) and washed with satd aqueous NH_4Cl solution (2 × 5 mL), and the combined aqueous layers were extracted with EtOAc (3 × 20 mL). The combined organic layers are washed with brine (5 mL), dried over $MgSO_4$, and concentrated. Flash silica gel chromatography using 15–30% EtOAc in hexanes gives the coupling product as a white solid.

General Cyclization Procedure A. To a solution of the Sonogashira coupling product (1 mmol) in anhydrous NMP (5 mL) was added KO*t*Bu (3.0 mmol), and the reaction was stirred under argon at room temperature for 17 h. The reaction mixture was diluted with Et_2O (30 mL) and washed with water (15 mL). The aqueous layer was extracted with Et_2O (3 × 20 mL), and the combined organic layers were washed with water (2 × 5 mL) and brine (5 mL), dried over $MgSO_4$, and concentrated. Flash silica gel chromatography using 0–10% MeOH in CH_2Cl_2 gives the diazaindole as a white solid.

General Cyclization Procedure B. To a solution of trifluoroacetyl protected aminopyridine (Sonogashira coupling product) (0.2 mmol) in anhydrous dioxane (0.8 mL) was added tetramethylguanidine (0.6 mmol) and the reaction mixture heated to 100 °C for 45 min. The reaction mixture was concentrated and purified using flash silica gel chromatography using 0–10% MeOH in CH_2Cl_2 or 0–100% EtOAc in hexanes to give the azaindole as a white solid.

5-Amino-4-bromopyrimidine (12). A solution of 5-amino-pyrimidine (3.00 g, 31.5 mmol) in CH_2Cl_2 (150 mL) and MeOH (30 mL) was treated with benzyltrimethylammonium tribromide (13.5 g, 34.7 mmol) in portions over a period of 10 min at 0 °C. The mixture was stirred for 15 min at 0 °C and then 90 min at room temperature. The mixture was treated with satd aqueous $NaHCO_3$ solution until the pH was approximately 8. The layers were separated. The aqueous layer was extracted with EtOAc (3 × 50 mL). The combined organic layers were dried over $MgSO_4$. The solvent was removed to give 5-amino-4-bromopyrimidine as an off-white solid which was used without further purification (51% yield). ^1H NMR (400 MHz, $CHCl_3$-*d*) δ 8.35 (s, 1H), 8.13 (s, 1H), 4.15 (br s, 2H).[19]

1,1,1-Trifluoro-4-methyl-pent-3-en-2-one (14). Step 1: To a 0–5 °C mixture of *N*,*O*-dimethylhydroxylamine hydrochloride (15.8 g) in CH_2Cl_2 (400 mL) was added dropwise trifluoroacetic anhydride (21.7 mL). Pyridine (37 mL) was added to the mixture dropwise. The resulting mixture was stirred at 0–5 °C for 0.5 h and diluted with water. The organic layer was washed with water, 1 N aqueous HCl, water, and brine and dried over $MgSO_4$. Removal of the volatiles in vacuo for 5 min provided 2,2,2-trifluoro-*N*-methoxy-*N*-methylacetamide as colorless oil.

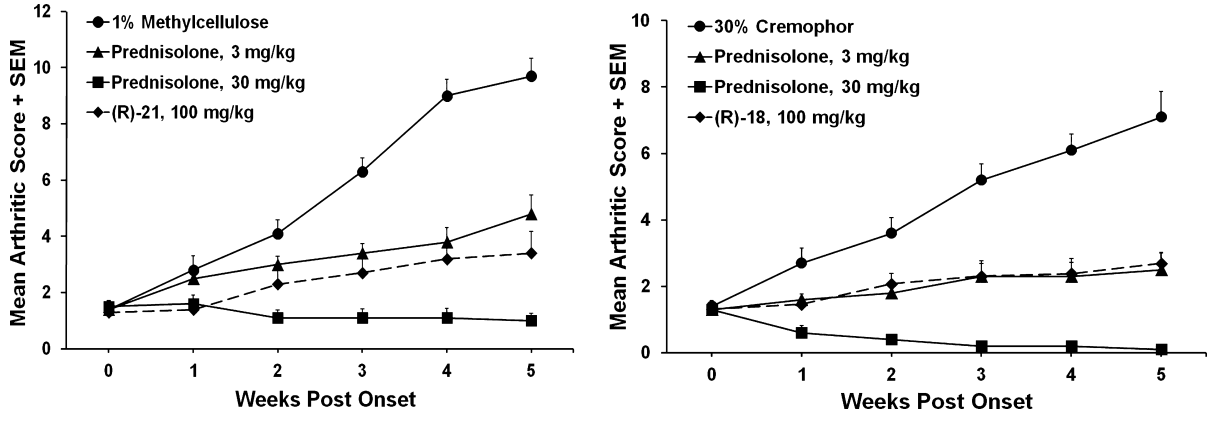

Figure 4. Collagen induced arthritis.

dx.doi.org/10.1021/jm4019178 | *J. Med. Chem.* 2014, 57, 1583–1598

Table 6. Side Effect Markers

compd and dose	CIA disease score AUC ± SE (% change vs vehicle)	body fat [%fat] mean ± SE (% change vs vehicle)	triglycerides [mEq/L] mean ± SE (% change vs vehicle)	free fatty acids [mEq/L] mean ± SE (% change vs vehicle)	insulin [ng/mL] mean ± SE (% change vs vehicle)
100 mg/kg (*R*)-**21**[c]	12.0 ± 2.0 (−57%)*[a]	23.0 ± 4.4 (+32%)	12.8 ± 6.5 (−14%)	1.45 ± 0.31 (+14%)**[b]	0.68 ± 0.43 (+17%)
3 mg/kg **2** (pred)[c]	15.8 ± 1.5 (−43%)*[a]	25.7 ± 2.8 (+48%)*[a]	18.0 ± 9.4 (+21%)	1.77 ± 0.19 (+39%)*[a]	0.94 ± 0.22 (+62%)*[a]
30 mg/kg **2** (pred)[c]	6.2 ± 1.3 (−78%)*[a]	29.3 ± 6.9 (+68%)*[a]	48.6 ± 41.5 (+226%)*[a]	1.83 ± 0.54 (+44%)*[a]	1.18 ± 0.94 (+103%)
100 mg/kg (*R*)-**18**[d]	10.2 ± 1.2 (−53%)*[a]	18.6 ± 2.6 (+8%)	NT	1.08 ± 0.24 (−2%)**[b]	0.25 ± 0.18 (−36%)
3 mg/kg **2** (pred)[d]	9.9 ± 1.5 (−55%)*[a]	22.8 ± 7.6 (+30%)	NT	1.43 ± 0.25 (+30%)*[a]	0.55 ± 0.72 (+36%)
30 mg/kg **2** (pred)[d]	2.1 ± 0.5 (−90%)*[a]	29.9 ± 6.1 (+71%)*[a]	NT	1.70 ± 0.44 (+54%)*[a]	3.17 ± 2.84 (+703%)*[a]

[a]*$p < 0.05$ vs vehicle. [b]**$p < 0.05$ vs pred at 3 mg/kg group. [c]From experiment 1: 1% methylcellulose vehicle. [d]From experiment 2: 30% cremophor vehicle.

Table 7. Bone Side Effects

compd and dose	CIA disease score AUC ± SE (% change vs vehicle)	femur cortical thickness [mm] mean ± SE (% change vs vehicle)
vehicle (1% methylcellulose)	27.8 ± 2.0	0.191 ± 0.002
100 mg/kg (*R*)-**21**[c]	12.0 ± 2.0 (−57%)*[a]	0.179 ± 0.002 (−6%)*[a]
3 mg/kg **2** (pred)[c]	15.8 ± 1.5 (−43%)*[a]	0.175 ± 0.002 (−9%)*[a]
30 mg/kg **2** (pred)[c]	6.2 ± 1.3 (−78%)*[a]	0.156 ± 0.002 (−18%)*[a]
vehicle (30% cremophor)	21.9 ± 1.6	0.189 ± 0.005
100 mg/kg (*R*)-**18**[d]	10.2 ± 1.2 (−53%)*[a]	0.174 ± 0.002 (−8%)*,***[a,b]
3 mg/kg **2** (pred)[d]	9.9 ± 1.5 (−55%)*[a]	0.165 ± 0.003 (−13%)*[a]
30 mg/kg **2** (pred)[d]	2.1 ± 0.5 (−90%)*[a]	0.147 ± 0.003 (−22%)*[a]

[a]*$p < 0.05$ vs vehicle. [b]**$p < 0.05$ vs pred at 3 mg/kg group. [c]From experiment 1: 1% methylcellulose vehicle. [d]From experiment 2: 30% cremophor vehicle.

Step 2: To a 0−5 °C mixture of 2,2,2-trifluoro-*N*-methoxy-*N*-methylacetamide (3.0 g) in anhydrous Et_2O (30 mL) was added 2-methylpropenylmagnesium bromide in THF (42 mL of a 0.5 M solution). The reaction was stirred at 0−5 °C for 0.5 h, warmed to room temperature, and stirred overnight. The reaction was quenched with satd aqueous NH_4Cl and extracted with Et_2O three times. The organic layers were combined and washed with water and brine and dried over $MgSO_4$. Most of the volatiles were removed at atmospheric pressure, and the resulting THF solution of 1,1,1-trifluoro-4-methyl-pent-3-en-2-one was used without further purification.

1,1,1-Trifluoro-4-(5-fluoro-2-methyl-phenyl)-4-methyl-pentan-2-one (16a). To a 0−5 °C cold solution of 1,1,1-trifluoro-4-methyl-pent-3-en-2-one (158 mmol, 75% in THF) and CuI (158 mmol) in Et_2O (300 mL) was added (5-fluoro-2-methyl-phenyl)-magnesium bromide solution (157 mL, 1 M in THF, 157 mmol). The mixture was warmed to room temperature, stirred overnight, and diluted with satd aqueous NH_4Cl solution (200 mL) and EtOAc. The organic layer was washed with water and brine and dried over $MgSO_4$. Removal of the volatiles in vacuo provided a residue which was purified by flash silica gel chromatography using 0−5% EtOAc in hexanes as the eluent to give 1,1,1-trifluoro-4-(5-fluoro-2-methyl-phenyl)-4-methyl-pentan-2-one (46% yield).

6-(5-Fluoro-2-methyl-phenyl)-6-methyl-4-trifluoromethyl-hept-1-yn-4-ol (17a). Aluminum amalgam was prepared from aluminum foil (1.16 g, 14.4 mmol) and mercuric chloride (12 mg, catalytic amount) in anhydrous THF (20 mL) by vigorously stirring the mixture at room temperature for 1 h under an argon atmosphere. A solution of propargyl bromide (4.80 mL, 80 wt % in toluene, 43.1 mmol) in anhydrous THF (25 mL) was slowly added to a stirred suspension maintaining a temperature of 30−40 °C, and stirring at 40 °C was continued until a dark-gray solution was obtained (1 h). The propargyl aluminum sesquibromide solution was added to a solution of 1,1,1-trifluoro-4-(5-fluoro-2-methyl-phenyl)-4-methyl-pentan-2-one (3.74 g, 14.4 mmol) in anhydrous Et_2O (150 mL) at −78 °C. The reaction mixture was stirred at this temperature for 3 h and then was allowed to warm to room temperature, at which time it was stirred for 12 h. The reaction mixture was then poured into ice water (20 mL) and extracted with Et_2O (4 × 30 mL). The combined extracts are washed with brine (20 mL), dried over $MgSO_4$, and concentrated. The residual oil was subjected to flash silica gel chromatography using 5−15% EtOAc in hexanes to give 6-(5-fluoro-2-methyl-phenyl)-6-methyl-4-trifluoromethyl-hept-1-yn-4-ol (99% yield) which was carried on to the next step without further purification.

The synthesis of enantiomerically pure **17a** (>98% *ee*) has been described elsewhere.[16,22]

6-(4-Fluoro-2-methoxy-phenyl)-6-methyl-4-trifluoromethyl-hept-1-yn-4-ol (17c). Step 1: A mixture of 1-(4-fluoro-2-hydroxy-phenyl)-ethanone (20 g, 0.13 mol), iodomethane (16 mL, 0.26 mol), K_2CO_3 (25 g, 0.18 mmol), and DMF (100 mL) was stirred at room temperature overnight. The mixture was poured into cold water (500 mL) and stirred for 15 min. The precipitate was collected by filtration, washed with water (3 × 500 mL), and dried under vacuum for 1 h to give 1-(4-fluoro-2-methoxy-phenyl)-ethanone (89% yield).

Step 2: A solution of 1-(4-fluoro-2-methoxy-phenyl)-ethanone (19.4 g, 0.12 mol) in toluene (170 mL) was treated with methyl cyanoacetate (15.2 mL, 0.17 mol), benzylamine (1.4 mL, 12 mmol), and acetic acid (6.6 mL, 0.10 mol). The mixture was heated to reflux with removal of water by Dean−Stark trap for 16 h. The solvent and remaining cyanoacetate were distilled off under high vacuum. The residue was flittered through a pad of silica gel using 10% EtOAc in a 1:1 mixture of CH_2Cl_2 and hexanes to give (*E*)-2-cyano-3-(4-fluoro-2-methoxy-phenyl)-but-2-enoic acid methyl ester (90% yield).

Step 3: A slurry of CuI (20 g, 0.11 mol) in Et_2O (350 mL) was stirred by overhead stirring and cooled to 0 °C. Methyl lithium (1.6 M in Et_2O, 120 mL, 0.19 mol) was added over 15 min, and the resulting mixture was allowed to stir at 0 °C for 10 min and then cooled to −15 °C. (*E*)-2-Cyano-3-(4-fluoro-2-methoxy-phenyl)-but-2-enoic acid methyl ester (12.1 g, 0.05 mol) in Et_2O (150 mL) was added over 20 min, and the reaction mixture was allowed to warm to room temperature. After 2 h, the reaction mixture was cautiously poured into aqueous NH_4Cl solution. Then 1 N HCl was added and the mixture was filtered through Celite and the layers separated. The aqueous layer was extracted with Et_2O (3 × 100 mL), and the combined organics were washed with 1 N HCl (100 mL), brine (100 mL), and aqueous $NaHCO_3$ (3 × 75 mL), dried over anhydrous $MgSO_4$, and concentrated to give 2-cyano-3-(4-fluoro-2-methoxy-phenyl)-3-methyl-butyric acid methyl ester (93% yield).

Step 4: To 2-cyano-3-(4-fluoro-2-methoxy-phenyl)-3-methyl-butyric acid methyl ester (12.0 g, 45 mmol) in DMSO (100 mL) were added NaCl (7.48 g, 130 mmol) and water (6 mL). The mixture was heated to reflux for 4 h. After cooling, brine (100 mL) was added and the mixture was extracted with EtOAc (4 × 100 mL). The combined organic extracts were washed with brine (4 × 100 mL), dried over anhydrous $MgSO_4$, and concentrated to give 3-(4-fluoro-2-methoxy-phenyl)-3-methyl-butyronitrile (98% yield).

Step 5: A solution of 3-(4-fluoro-2-methoxy-phenyl)-3-methyl-butyronitrile (9.2 g, 44 mmol) in CH_2Cl_2 (180 mL) was cooled to −40 °C. DIBAL-H (1 M in CH_2Cl_2, 91 mL, 91 mmol) was added over 10 min. The reaction mixture was allowed to warm to room temperature and stirred for 16 h. The mixture was cautiously added to 1 N HCl and

dx.doi.org/10.1021/jm4019178 | J. Med. Chem. 2014, 57, 1583−1598

the phases separated. The aqueous layer was extracted with CH_2Cl_2 (2 × 100 mL), the combined organic extracts were washed with 1 N HCl (100 mL), brine (2 × 100 mL), and $NaHCO_3$ solution (100 mL), dried over anhydrous $MgSO_4$, filtered, and concentrated to give 3-(4-fluoro-2-methoxy-phenyl)-3-methyl-butyraldehyde (88% yield).

Step 6: 3-(4-Fluoro-2-methoxy-phenyl)-3-methyl-butyraldehyde (8.13 g, 39 mmol) was dissolved in THF (100 mL) and treated with trifluoromethyl trimethylsilane (7.8 g, 55 mmol). Tetrabutylammonium fluoride (1 M in THF, 8.5 mL) was added dropwise. The reaction mixture was stirred 30 min, and additional tetrabutylammonium fluoride (1 M in THF, 34.5 mL) was added. The reaction mixture was diluted with water and extracted with EtOAc (3 × 100 mL). The combined organic extracts were washed with 1 N HCl (3 × 100 mL), brine (3 × 100 mL), and $NaHCO_3$ solution (3 × 100 mL), dried over $MgSO_4$, filtered, and concentrated to give 1,1,1-trifluoro-4-(4-fluoro-2-methoxy-phenyl)-4-methyl-pentan-2-ol (96% yield).

Step 7: To 1,1,1-trifluoro-4-(4-fluoro-2-methoxy-phenyl)-4-methyl-pentan-2-ol (10.5 g, 38 mmol) in CH_2Cl_2 (180 mL) Dess–Martin periodinane (22.5 g, 53 mmol) was added and the mixture allowed to stir for 1 h. The reaction mixture was passed through a pad of silica eluting with hexane to give 1,1,1-trifluoro-4-(4-fluoro-2-methoxy-phenyl)-4-methyl-pentan-2-one as a pale-yellow crystalline solid (81% yield).

Step 8: Aluminum foil (226 mg, 8.4 mmol) was cut into small pieces and stirred with $HgCl_2$ (5 mg, 0.02 mmol) and THF (5 mL) at room temperature for 1 h. Propargylbromide (80% in toluene, 0.94 mL, 8.4 mmol) was added dropwise, and the mixture was stirred for 2 h at 40 °C. This suspension was added to a solution of 1,1,1-trifluoro-4-(4-fluoro-2-methoxy-phenyl)-4-methyl-pentan-2-one (1.00 g, 3.6 mmol) in Et_2O (20 mL) at −78 °C. The mixture was warmed to room temperature. After 2 h, NH_4Cl solution (20 mL) and EtOAc (50 mL) were added. The organic phase was separated, and the aqueous layer was extracted with EtOAc (100 mL). The combined organic phases were dried over $MgSO_4$. The solvent was removed to give **17c** as an oil that was used as such (96% yield).

6-(2-Methanesulfonyl-phenyl)-6-methyl-4-trifluoromethyl-hept-1-yn-4-ol (17d). Step 1: Magnesium turnings (290 mg, 11.8 mmol) under THF (20 mL) were treated with 1-bromo-2-methylsulfanyl-benzene (2.00 g, 9.85 mmol) in one portion, and the resulting mixture was heated to 90 °C for 3 h. The reaction was cooled to −10 °C. With stirring, CuI (2.06 g, 10.8 mmol) was added and the resulting mixture was stirred at that temperature for 1 h. 1,1,1-Trifluoro-4-methyl-pent-3-en-2-one (2.75 g, 60% in THF, 10.8 mmol) was added, and the mixture was allowed to warm to room temperature and stirred for 16 h. The reaction was poured into rapidly stirring satd aqueous NH_4Cl solution, diluted with Et_2O, and the layers were separated. The aqueous layer was extracted with Et_2O (2 × 50 mL). The combined organic phases were dried over $MgSO_4$, filtered, and concentrated. The resulting oil was purified by flash chromatography on silica gel using 0–10% EtOAc in hexanes to give 1,1,1-trifluoro-4-methyl-4-(2-methylsulfanyl-phenyl)-pentan-2-one as an orange oil (42% yield).

Step 2: To a solution of 1,1,1-trifluoro-4-methyl-4-(2-methylsulfanyl-phenyl)-pentan-2-one (1.14 g, 4.13 mmol) in CH_3CN/water (3:1, 80 mL) was added $NaIO_4$ (2.65 g, 12.4 mmol), followed by the addition of $RuCl_3$ (17 mg, 0.08 mmol), and the reaction was stirred at room temperature. After 30 min, the reaction was diluted with water and extracted with CH_2Cl_2 (3 × 50 mL). The organic phases were combined, dried over $MgSO_4$, and concentrated. The black residue was purified by flash chromatography on silica gel using 30–100% EtOAc in hexanes to give 1,1,1-trifluoro-4-(2-methanesulfonyl-phenyl)-4-methyl-pentan-2-one as a colorless oil (74% yield).

Step 3: Aluminum foil (250 mg, 9.2 mmol) was cut into small pieces and stirred with $HgCl_2$ (17 mg, 0.06 mmol) and THF (6 mL) at 0 °C for 10 min. Propargylbromide (80% in toluene, 1.03 mL, 9.2 mmol) was added dropwise, and the mixture was stirred for 1 h at 50 °C. This suspension was added to a solution of 1,1,1-trifluoro-4-(2-methanesulfonyl-phenyl)-4-methyl-pentan-2-one (947 mg, 3.07 mmol) in THF (10 mL) at −78 °C. The mixture was warmed to room temperature. After 2 h, NH_4Cl solution (10 mL) and Et_2O (50 mL) were added. The organic phase was separated, and the aqueous layer was extracted with Et_2O (3 × 100 mL). The combined organic phases were dried over Na_2SO_4 and concentrated. The residue was purified by flash chromatography using 0–30% EtOAc in hexanes to give **17d** as a yellow oil (94% yield).

6-(3-Methanesulfonyl-phenyl)-6-methyl-4-trifluoromethyl-hept-1-yn-4-ol (17e). **17e** was prepared in analogy to **17d** in three steps in an overall yield of 31% using 1-bromo-3-methylsulfanyl-benzene instead of 1-bromo-2-methylsulfanyl-benzene in step 1.

1,1,1-Trifluoro-4-(5-fluoro-2-methyl-phenyl)-4-methyl-2-(5*H*-pyrrolo[3,2-*c*]pyridazin-6-ylmethyl)-pentan-2-ol (18) and 1,1,1-Trifluoro-4-(5-fluoro-2-methyl-phenyl)-4-methyl-2-(1*H*-pyrrolo[2,3-*d*]pyridazin-2-ylmethyl)-pentan-2-ol (19). Following the general Sonogashira coupling procedure starting from **17a** and a 1:1 mixture of **9** and **10**[19] gave a 1:1 mixture of 1-(4-amino-pyridazin-3-yl)-6-(5-fluoro-2-methyl-phenyl)-6-methyl-4-trifluoromethyl-hept-1-yn-4-ol and 1-(5-amino-pyridazin-4-yl)-6-(5-fluoro-2-methyl-phenyl)-6-methyl-4-trifluoromethyl-hept-1-yn-4-ol (yield 44%).

Following the general cyclization procedure A starting from a 1:1 mixture of 1-(4-amino-pyridazin-3-yl)-6-(5-fluoro-2-methyl-phenyl)-6-methyl-4-trifluoromethyl-hept-1-yn-4-ol and 1-(5-amino-pyridazin-4-yl)-6-(5-fluoro-2-methyl-phenyl)-6-methyl-4-trifluoromethyl-hept-1-yn-4-ol gave **18** (less polar product) as a white solid (16% yield) and **19** (more polar product) as a white solid (35% yield).

18: ^{1}H NMR (400 MHz, MeOH-d_4) δ 8.74 (d, J = 6 Hz, 1H), 7.55 (dd, J = 6 Hz, J = 1 Hz, 1H), 7.18 (dd, J = 12 Hz, J = 1 Hz, 1H), 7.07–7.10 (m, 1H), 6.78–6.82 (m, 1H), 6.49 (s, 1H), 2.88 (d, J = 15 Hz, 1H), 2.77 (d, J = 15 Hz, 1H), 2.62 (d, J = 16 Hz, 1H), 2.50 (s, 3H), 2.13 (d, J = 16 Hz, 1H), 1.70 (s, 3H), 1.46 (s, 3H).

19: ^{1}H NMR (400 MHz, MeOH-d_4) δ 9.18 (d, J = 1 Hz, 1H), 9.11 (s, 1H), 7.17 (dd, J = 12 Hz, J = 2 Hz, 1H), 7.07–7.11 (m, 1H), 6.78–6.82 (m, 1H), 6.37 (s, 1H), 2.87 (d, J = 15 Hz, 1H), 2.74 (d, J = 15 Hz, 1H), 2.61 (d, J = 15 Hz, 1H), 2.50 (s, 3H), 2.12 (d, J = 16 Hz, 1H), 1.70 (s, 3H), 1.45 (s, 3H).

The pure enantiomer (*R*)-**18** was synthesized following the same sequence outlined in Scheme 1 using enantiopure alkyne **11a**.[16,22] Chiral HPLC (Chiral APG 150X column, 4.0 mm, 5 μm; mobile phase 20 nM NH_4OAc/acetonitrile 82:18 isocratic) rf 5.07 min, (*S*)-**18** 7.62 min; *ee* 99.6%. HRMS: $(M + H)^+$ 396.1700 (calcd 396.1704).

1,1,1-Trifluoro-4-(5-fluoro-2-methyl-phenyl)-4-methyl-2-(3-phenyl-7*H*-pyrrolo[2,3-*c*]pyridazin-6-ylmethyl)-pentan-2-ol (20). Following the general Sonogashira coupling procedure starting from **17a** and **11**[20] gave 1-(3-amino-6-phenyl-pyridazin-4-yl)-6-(5-fluoro-2-methyl-phenyl)-6-methyl-4-trifluoromethyl-hept-1-yn-4-ol (32% yield).

Following the general cyclization procedure A starting from 1-(3-amino-6-phenyl-pyridazin-4-yl)-6-(5-fluoro-2-methyl-phenyl)-6-methyl-4-trifluoromethyl-hept-1-yn-4-ol gave **20** after recrystallization from Et_2O as a white solid (27% yield). ^{1}H NMR (400 MHz, MeOH-d_4) δ 8.08 (s, 1H), 7.96–7.98 (m, 2H), 7.50–7.54 (m, 2H), 7.43–7.47 (m, 1H), 7.21 (dd, J = 12 Hz, J = 2 Hz, 1H), 7.10 (dd, J = 8 Hz, J = 6 Hz, 1H), 6.83 (td, J = 8 Hz, J = 2 Hz, 1H), 6.31 (s, 1H), 2.95 (d, J = 15 Hz, 1H), 2.77 (d, J = 16 Hz, 1H), 2.68 (d, J = 15 Hz, 1H), 2.52 (s, 3H), 2.19 (d, J = 16 Hz, 1H), 1.49 (s, 3H), 1.19 (s, 3H).

1,1,1-Trifluoro-4-(5-fluoro-2-methyl-phenyl)-4-methyl-2-(5*H*-pyrrolo[3,2-*d*]pyrimidin-6-ylmethyl)-pentan-2-ol (21). Following the general Sonogashira coupling procedure starting from **17a** and **12** gave 1-(5-amino-pyrimidin-4-yl)-6-(5-fluoro-2-methyl-phenyl)-6-methyl-4-trifluoromethyl-hept-1-yn-4-ol (47% yield).

Following the general cyclization procedure A starting from 1-(5-amino-pyrimidin-4-yl)-6-(5-fluoro-2-methyl-phenyl)-6-methyl-4-trifluoromethyl-hept-1-yn-4-ol gave **21** as a white solid (15% yield). ^{1}H NMR (400 MHz, MeOH-d_4) δ 8.70 (s, 1H), 8.67 (s, 1H), 7.17 (dd, J = 12 Hz, J = 2 Hz, 1H), 7.06–7.10 (m, 1H), 6.79–6.83 (m, 1H), 6.29 (s, 1H), 2.90 (d, J = 15 Hz, 1H), 2.75 (d, J = 15 Hz, 1H), 2.63 (d, J = 15 Hz, 1H), 2.50 (s, 3H), 2.13 (d, J = 16 Hz, 1H), 1.70 (s, 3H), 1.45 (s, 3H).

The pure enantiomer (*R*)-**21** was synthesized following the same sequence outlined in Scheme 1 using enantiopure alkyne **11a**.[16,22] Chiral HPLC (Chiral APG 150X column, 4.0 mm, 5 μm; mobile phase

20 nM NH_4OAc/acetonitrile 82:18 isocratic) rf 4.65 min, (*S*)-**21** 7.03 min; *ee* 99.4%. HRMS: $(M + H)^+$ 396.1704 (calcd 396.1704). Elemental analysis: C, 60.67% (calcd 60.75%); H, 5.38% (calcd 5.35%); N, 10.35% (calcd 10.63%); F, 19.38% (calcd 19.22%).

1,1,1-Trifluoro-4-(5-fluoro-2-methoxy-phenyl)-4-methyl-2-(7*H*-pyrrolo[2,3-*d*]pyrimidin-6-ylmethyl)-pentan-2-ol (22). Step 1: Following the general Sonogashira coupling procedure starting from **17b**[16] and **12**[19] gave 1-(4-amino-pyrimidin-5-yl)-6-(5-fluoro-2-methoxy-phenyl)-6-methyl-4-trifluoromethyl-hept-1-yn-4-ol (50% yield).

Step 2: 1-(4-Amino-pyrimidin-5-yl)-6-(5-fluoro-2-methoxy-phenyl)-6-methyl-4-trifluoromethyl-hept-1-yn-4-ol (150 mg, 0.37 mmol) was dissolved in CH_2Cl_2 (5 mL). At 0 °C, pyridine (0.09 g, 1.1 mmol) was added, followed by slow addition of acetyl chloride (0.06 g, 0.73 mmol), and the mixture was stirred for 1 h. The reaction mixture was diluted with CH_2Cl_2 and washed with brine (3 × 10 mL). The residue was purified by flash chromatography on silica gel using 3% MeOH in CH_2Cl_2 to give slightly impure *N*-{5-[6-(5-fluoro-2-methoxy-phenyl)-4-hydroxy-6-methyl-4-trifluoromethyl-hept-1-ynyl]-pyrimidin-4-yl}-acetamide (75% yield).

Step 3: *N*-{5-[6-(5-fluoro-2-methoxy-phenyl)-4-hydroxy-6-methyl-4-trifluoromethyl-hept-1-ynyl]-pyrimidin-4-yl}-acetamide (125 mg, 0.28 mmol) was dissolved in DMSO (0.5 mL) and treated with tetramethylguanidine (0.10 g, 0.83 mmol). The mixture was heated in the microwave at 140 °C for 10 min. The reaction mixture was then diluted with EtOAc (10 mL) and washed with water (3 × 5 mL). The organic phase was separated, dried over $MgSO_4$, filtered, and concentrated. The residue was purified by reversed phase HPLC using 35−100% CH_3CN in water to give **22** as a white solid (23% yield). ^{1}H NMR (400 MHz, $CHCl_3$-*d*) δ 9.31 (br s, 1H), 8.87 (s, 1H), 8.78 (s, 1H), 7.02 (dd, *J* = 10 Hz, *J* = 2 Hz, 1H), 6.91−6.94 (m, 1H), 6.80−6.83 (m, 1H), 6.26 (s, 1H), 3.74 (s, 3H), 2.98 (s, 2H), 2.49 (s, 2H), 1.49 (s, 3H), 1.38 (s, 3H). No analytical HPLC data.

1,1,1-Trifluoro-4-(5-fluoro-2-methyl-phenyl)-4-methyl-2-(5*H*-pyrrolo[2,3-*b*]pyrazin-6-ylmethyl)-pentan-2-ol (23). Following the general Sonogashira coupling procedure starting from **17a** and **13a**[21] gave 1-(3-amino-pyrazin-2-yl)-6-(5-fluoro-2-methyl-phenyl)-6-methyl-4-trifluoromethyl-hept-1-yn-4-ol (54% yield).

Following the general cyclization procedure A starting from 1-(3-amino-pyrazin-2-yl)-6-(5-fluoro-2-methyl-phenyl)-6-methyl-4-trifluoromethyl-hept-1-yn-4-ol gave **23** as a white solid (18% yield). ^{1}H NMR (400 MHz, MeOH-d_4) δ 8.14 (d, *J* = 3 Hz, 1H), 8.04 (d, *J* = 3 Hz, 1H), 7.07 (dd, *J* = 12 Hz, *J* = 3 Hz, 1H), 6.94 (dd, *J* = 8 Hz, *J* = 7 Hz, 1H), 6.69 (td, *J* = 8 Hz, *J* = 3 Hz, 1H), 6.21 (s, 1H), 2.82 (d, *J* = 15 Hz, 1H), 2.60 (d, *J* = 16 Hz, 1H), 2.59 (d, *J* = 15 Hz, 1H), 2.38 (s, 3H), 2.06 (d, *J* = 16 Hz, 1H), 1.57 (s, 3H), 1.36 (s, 3H).

1,1,1-Trifluoro-4-(5-fluoro-2-methyl-phenyl)-4-methyl-2-(2-phenyl-5*H*-pyrrolo[2,3-*b*]pyrazin-6-ylmethyl)-pentan-2-ol (24b). Following the general Sonogashira coupling procedure starting from **17a** and **13b** gave 1-(3-amino-6-bromo-pyrazin-2-yl)-6-(5-fluoro-2-methyl-phenyl)-6-methyl-4-trifluoromethyl-hept-1-yn-4-ol (75% yield).

Following the general cyclization procedure A starting from 1-(3-amino-6-bromo-pyrazin-2-yl)-6-(5-fluoro-2-methyl-phenyl)-6-methyl-4-trifluoromethyl-hept-1-yn-4-ol gave 2-(2-bromo-5*H*-pyrrolo[2,3-*b*]-pyrazin-6-ylmethyl)-1,1,1-trifluoro-4-(5-fluoro-2-methyl-phenyl)-4-methyl-pentan-2-ol (36% yield).

Step 3: 2-(2-Bromo-5*H*-pyrrolo[2,3-*b*]pyrazin-6-ylmethyl)-1,1,1-trifluoro-4-(5-fluoro-2-methyl-phenyl)-4-methyl-pentan-2-ol (50 mg, 0.11 mmol) was dissolved in DME/MeOH/DMF (1 mL, 0.5 mL, 1.5 mL). $Pd(PPh_3)_4$ (12 mg, 0.01 mmol), phenylboronic acid (26 mg, 0.22 mmol), and K_2CO_3 (43 mg, 0.33 mmol) were added, and the mixture was heated for 3 h to 80 °C. NaOH (1 M, 5 mL) was added. The reaction mixture was diluted with EtOAc (20 mL). The organic phase was separated, and the aqueous phase was extracted with EtOAc (3 × 20 mL). The combined organic extracts were dried over $MgSO_4$ and the solvent evaporated. The residue was purified by flash chromatography on silica gel using 0−50% hexanes in EtOAc to give impure product as a solid. The material was repurified by preparative TLC (50% hexanes in EtOAc) to give pure product **24b** as a white solid (71% yield). ^{1}H NMR (400 MHz, MeOH-d_4) δ 8.48 (s, 1H), 7.84−7.86 (m, 2H), 7.38−7.42 (m, 2H), 7.30−7.34 (m, 1H), 7.08 (dd, *J* = 12 Hz, *J* = 3 Hz, 1H), 6.95 (dd, *J* = 8 Hz, *J* = 7 Hz, 1H), 6.70 (td, *J* = 8 Hz, *J* = 3 Hz, 1H), 6.26 (s, 1H), 2.85 (d, *J* = 15 Hz, 1H), 2.62 (d, *J* = 16 Hz, 1H), 2.60 (d, *J* = 15 Hz, 1H), 2.39 (s, 3H), 2.08 (d, *J* = 16 Hz, 1H), 1.58 (s, 3H), 1.37 (s, 3H).

***N*-(4-Chloro-2-pyridin-3-yl-pyrimidin-5-yl)-2,2,2-trifluoro-acetamide (25c).** Step 1: Ethylnitro acetate (5.6 mL, 50 mmol) and *N*,*N*-dimethylformamide dimethyl acetal (6.6 mL, 50 mmol) were stirred for 45 min at room temperature and then heated to 90 °C for 15 min. After cooling, the obtained (*Z*)-3-dimethylamino-2-nitro-acrylic acid ethyl ester was used directly in the next step.

Step 2: A mixture of (*Z*)-3-dimethylamino-2-nitro-acrylic acid ethyl ester (9.4 g, 50 mmol), 3-pyridyl amidine hydrochloride (4.7 g, 30 mmol), and K_2CO_3 (4.1 g, 30 mmol) in anhydrous ethanol (30 mL) was heated to 90 °C for 8 h. A yellowish solid precipitated from the reaction mixture which was filtered, washed with Et_2O, and dried to give 5-nitro-2-pyridin-3-yl-3*H*-pyrimidin-4-one as a yellowish solid (92% yield). This material contained residual potassium salts and was used as such in the next step.

Step 3: A stirred solution of DMF (6.8 mL, 88 mmol) in CH_2Cl_2 (100 mL) was cooled to 0 °C. $POCl_3$ (8.2 mL, 88 mmol) in CH_2Cl_2 (50 mL) was added, and stirring was continued for 30 min. 5-Nitro-2-pyridin-3-yl-3*H*-pyrimidin-4-one (5.4 g, 70%, 18 mmol) was added and the mixture stirred for 1 h. The reaction mixture was diluted with CH_2Cl_2 (200 mL), treated with ice and solid $KHCO_3$. The organic layer was separated, washed with water, dried over anhydrous Na_2SO_4, and concentrated to give a reddish oil. This material was taken up in cold water, a solid precipitated which was filtered, washed with water, and dried to give 4-chloro-5-nitro-2-pyridin-3-yl-pyrimidine as an orange solid (41% yield).

Step 4: 4-Chloro-5-nitro-2-pyridin-3-yl-pyrimidine (480 mg, 2 mmol) was stirred in concentrated HCl (6 mL) at room temperature until a clear solution was obtained. Acetic acid (3 mL) was added. Tin(II) chloride dihydrate (1.8 g, 8.0 mmol) in 3 mL of concentrated HCl was slowly added over a period of 5 min. The reaction mixture was stirred at room temperature for 18 h. At 0 °C, the reaction mixture was treated with 10 N KOH solution until the pH of the reaction mixture was 8−9. The mixture was extracted with EtOAc (4 × 75 mL). The combined extracts were dried over anhydrous Na_2SO_4 and solvent evaporated to give 4-chloro-2-pyridin-3-yl-pyrimidin-5-ylamine as a light-yellow thick oil that was used as was in the next step.

Step 5: To a solution of 4-chloro-2-pyridin-3-yl-pyrimidin-5-ylamine (413 mg, 2 mmol) in CH_2Cl_2 (8 mL) at room temperature was added a solution of trifloroacetic anhydride (0.56 mL, 4 mmol) in CH_2Cl_2 (2 mL). The reaction mixture was stirred for 30 min. The solvent was removed to give a thick oil that was purified by flash chromatography on silica gel using 0−100% EtOAc in CH_2Cl_2 to give **25c** as an off-white crystalline solid (56% yield over two steps).

2,2,2-Trifluoro-*N*-(4-iodo-2-pyrrolidin-1-yl-pyrimidin-5-yl)-acetamide (25d). Step 1 is identical to step 1 described for **25c**. Step 2: To a stirred solution of (*Z*)-3-dimethylamino-2-nitro-acrylic acid ethyl ester (3.5 g, 20 mmol) in trifluoroethanol (50 mL) was added pyrrolidinoamidine hydrochloride (4.8 g, 20 mmol) followed by triethylamine (2.0 mL, 20 mmol), and the mixture was heated to 90 °C for 6 h. After cooling, the reaction mixture was concentrated and the residue was purified by flash chromatography using 5% MeOH in CH_2Cl_2 to give 5-nitro-2-pyrrolidin-1-yl-3*H*-pyrimidin-4-one as a light-yellow solid (50% yield).

Step 3: A stirred solution of DMF (1.6 mL, 20 mmol) in CH_2Cl_2 (20 mL) was cooled to 0 °C. $POCl_3$ (1.9 mL, 20 mmol) was added, and stirring was continued for 30 min. 5-Nitro-2-pyrrolidin-1-yl-3*H*-pyrimidin-4-one (2.1 g, 10 mmol) was added and the mixture stirred for 10 min. The reaction mixture was diluted with CH_2Cl_2 (100 mL) and treated with ice and solid $KHCO_3$. The organic layer was separated, washed with water, dried over anhydrous Na_2SO_4, and concentrated to give a brown oil that was purified by flash chromatography on silica gel using 25% EtOAc in hexanes to give 4-chloro-5-nitro-2-pyrrolidin-1-yl-pyrimidine as an off-white solid (36% yield).

dx.doi.org/10.1021/jm4019178 | *J. Med. Chem.* 2014, 57, 1583−1598

Step 4: To 4-chloro-5-nitro-2-pyrrolidin-1-yl-pyrimidine (0.82 g, 3.6 mmol) in EtOH (15 mL) and glacial acetic acid (7 mL) was added iron powder (2.0 g, 36 mmol), and the mixture was heated to 90 °C for 20 min. After cooling to room temperature, the reaction mixture was diluted with CH_2Cl_2 (250 mL) and filtered through Celite. The filtrate was washed with $NaHCO_3$ solution (50 mL) and water (50 mL), dried over anhydrous Na_2SO_4, and the solvent was evaporated to give 4-chloro-2-pyrrolidin-1-yl-pyrimidin-5-ylamine as a bluish thick oil that was used for the next reaction as is (84% yield).

Step 5: To a stirred mixture of 4-chloro-2-pyrrolidin-1-yl-pyrimidin-5-ylamine (0.60 g, 3.0 mmol) in 40% aqueous hydroiodic acid (15 mL, 120 mmol) was added NaI (2.26 g, 15 mmol). The mixture was stirred at room temperature for 4 h and then poured into EtOAc (200 mL) and washed with aqueous Na_2CO_3 solution, followed by sodium bisulfite solution and water. The organic layer was dried over anhydrous Na_2SO_4 and concentrated to give 4-iodo-2-pyrrolidin-1-yl-pyrimidin-5-ylamine as an oil which slowly solidified (97% yield).

Step 6: To a stirred solution of 4-iodo-2-pyrrolidin-1-yl-pyrimidin-5-ylamine (850 mg, 2.9 mmol) in CH_2Cl_2 (5 mL) at room temperature was added a solution of trifluoroacetic anhydride (0.62 mL, 4.4 mmol) in CH_2Cl_2 (2 mL) After 15 min, the solvent was evaporated to give **25d** as a brownish solid that was used as is in the next reaction (93% yield).

2,2,2-Trifluoro-*N*-(4-chloro-2-morpholin-4-yl-pyrimidin-5-yl)-acetamide (25e). **25e** was prepared in analogy to **25c** in five steps in 15% overall yield from ethylnitroacetate and dimethyl formamide dimethyl acetal using morpholinoamidine hydrochloride instead of 3-pyridyl amidine hydrochloride in step 2.

***N*-[4-Chloro-2-(1,1-dioxo-1λ6-thiomorpholin-4-yl)-pyrimidin-5-yl]-2,2,2-trifluoro-acetamide (25f).** Step 1: 2-Chloro-5-nitro-pyrimidine (4.00 g, 25 mmol) was stirred in CH_3CN (40 mL) and THF (10 mL) until a clear solution was obtained. Thiomorpholine (2.06 g, 25 mmol) in CH_3CN (5 mL) was added. A yellowish solid precipitated. After 10 min, a solution of $NaHCO_3$ (26 mmol) in water was added and the reaction mixture was stirred at room temperature for 45 min. The solvent was removed and the residue taken up in cold water. The solid was collected by filtration and dried to give 4-(5-nitro-pyrimidin-2-yl)-thiomorpholine as a yellowish solid (99% yield).

Step 2: 4-(5-Nitro-pyrimidin-2-yl)-thiomorpholine (2.7 g, 12 mmol) was stirred in concentrated HCl (10 mL) at room temperature until a clear solution was obtained. Tin(II) chloride (10.8 g, 48 mmol) in concentrated HCl (10 mL) was added over a period of 15 min. A yellow solid precipitated. The reaction mixture was diluted with water (300 mL) and EtOAc (400 mL). The stirred mixture was neutralized with solid $NaHCO_3$ until the pH was 6−7 and filtered. The organic fraction of the filtrate was separated. The aqueous fraction was extracted with EtOAc (2 × 150 mL). The combined organic fractions were washed with brine, dried over anhydrous Na_2SO_4, and the solvent evaporated to give a reddish thick oil which was purified by flash chromatography on silica gel using 0−100% EtOAc in hexanes to give 4-chloro-2-thiomorpholin-4-yl-pyrimidin-5-ylamine (20% yield) and 2-thiomorpholin-4-yl-pyrimidin-5-ylamine (14% yield).

Step 3: To a solution of 4-chloro-2-thiomorpholin-4-yl-pyrimidin-5-ylamine (540 mg, 2.3 mmol) in CH_2Cl_2 (7 mL) at 0 °C was added a solution of the trifloroacetic anhydride (0.42 mL, 3.0 mmol) in CH_2Cl_2 (3 mL). The reaction mixture was allowed to stand at room temperature. After 30 min, the solvent was removed to give a thick oil that was purified by flash chromatography on silica gel using 0−30% EtOAc in hexanes to give *N*-(4-chloro-2-thiomorpholin-4-yl-pyrimidin-5-yl)-2,2,2-trifluoro-acetamide as a light-yellow solid (75% yield).

Step 4: To a solution of *N*-(4-chloro-2-thiomorpholin-4-yl-pyrimidin-5-yl)-2,2,2-trifluoro-acetamide (570 mg, 1.7 mmol) in CH_3CN (10 mL) was added a solution of $NaIO_4$ (0.93 g, 4.4 mmol) in water (3 mL), and the reaction mixture was stirred at room temperature. After 1 h, $RuCl_3$ hydrate (15 mg, 0.1 mmol) was added and the reaction mixture was stirred for 15 min. The reaction was diluted with water and extracted with CH_2Cl_2. The combined organic extracts were dried over Na_2SO_4 and concentrated. The residue was filtered through Celite and concentrated to give **25f** as a thick oil (67% yield).

1,1,1-Trifluoro-4-(5-fluoro-2-methyl-phenyl)-2-(2-isopropyl-5*H*-pyrrolo[3,2-*d*]pyrimidin-6-ylmethyl)-4-methyl-pentan-2-ol (26). Following the general Sonogashira coupling procedure starting from **17a** and **25a**[19] gave 2,2,2-trifluoro-*N*-{4-[6-(5-fluoro-2-methyl-phenyl)-4-hydroxy-6-methyl-4-trifluoromethyl-hept-1-ynyl]-2-isopropyl-pyrimidin-5-yl}-acetamide (38% yield).

Following the general cyclization procedure B starting from 2,2,2-trifluoro-*N*-{4-[6-(5-fluoro-2-methyl-phenyl)-4-hydroxy-6-methyl-4-trifluoromethyl-hept-1-ynyl]-2-isopropyl-pyrimidin-5-yl}-acetamide gave **27** as a white solid (33% yield). ^{1}H NMR (400 MHz, DMSO-d_6) δ 11.17 (s, 1H), 8.68 (d, J = 1 Hz, 1H), 7.09−7.14 (m, 2H), 6.91 (td, J = 8 Hz, J = 3 Hz, 1H), 6.22 (s, 1H), 6.15 (s, 1H), 3.12 (sept, J = 7 Hz, 1 H), 2.84 (d, J = 15 Hz, 1H), 2.65 (d, J = 15 Hz, 1H), 2.48 (d, J = 15 Hz, 1H), 2.43 (s, 3H), 2.15 (d, J = 15 Hz, 1H), 1.57 (s, 3H), 1.40 (s, 3H), 1.26 (d, J = 7 Hz, 6H).

1,1,1-Trifluoro-4-(5-fluoro-2-methyl-phenyl)-4-methyl-2-(2-phenyl-5*H*-pyrrolo[3,2-*d*]pyrimidin-6-ylmethyl)-pentan-2-ol (27). Following the general Sonogashira coupling procedure starting from **17a** and **25b**[19] gave 2,2,2-trifluoro-*N*-{4-[6-(5-fluoro-2-methyl-phenyl)-4-hydroxy-6-methyl-4-trifluoromethyl-hept-1-ynyl]-2-phenyl-pyrimidin-5-yl}-acetamide (56% yield).

Following the general cyclization procedure B starting from 2,2,2-trifluoro-*N*-{4-[6-(5-fluoro-2-methyl-phenyl)-4-hydroxy-6-methyl-4-trifluoromethyl-hept-1-ynyl]-2-phenyl-pyrimidin-5-yl}-acetamide gave **27** as a white solid (60% yield). ^{1}H NMR (400 MHz, DMSO-d_6) δ 11.51 (s, 1H), 8.98 (s, 1H), 8.46−8.48 (m, 2H), 7.45−7.55 (m, 3H), 7.16−7.22 (m, 2H), 6.97 (td, J = 8 Hz, J = 3 Hz, 1H), 6.44 (s, 1H), 6.31 (s, 1H), 2.96 (d, J = 15 Hz, 1H), 2.77 (d, J = 15 Hz, 1H), 2.56−2.60 (m, 1H), 2.50 (s, 3H), 2.23 (d, J = 15 Hz, 1H), 1.64 (s, 3H), 1.48 (s, 3H).

1,1,1-Trifluoro-4-(5-fluoro-2-methyl-phenyl)-4-methyl-2-(2-pyridin-3-yl-5*H*-pyrrolo[3,2-*d*]pyrimidin-6-ylmethyl)-pentan-2-ol (28). A solution of the alkyne **17a** (151 mg, 0.50 mmol) and the chloropyrimidine **25c** (91 mg, 0.30 mmol) in CH_3CN (0.7 mL) and triethylamine (0.2 mL) was degassed by bubbling argon through for 5 min. $Pd(PPh_3)_2Cl_2$ (21 mg, 0.03 mmol) and CuI (5.7 mg, 0.03 mmol) were added. The reaction mixture was heated to 70 °C for 2 h. The reaction mixture was subjected to flash chromatography on silica gel using 0−100% EtOAc in CH_2Cl_2 to give **28** as an off-white solid (57% yield). ^{1}H NMR (400 MHz, DMSO-d_6) δ 11.49 (s, 1H), 9.53 (s, 1H), 8.91 (s, 1H), 8.67 (td, J = 4 Hz, J = 2 Hz, 1H), 8.61 (d, J = 4 Hz, 1H), 7.50 (dd, J = 8 Hz, J = 5 Hz, 1H), 7.11−7.16 (m, 2H), 6.91 (td, J = 8 Hz, J = 3 Hz, 1H), 6.42 (s, 1H), 6.24 (s, 1H), 2.89 (d, J = 15 Hz, 1H), 2.71 (d, J = 15 Hz, 1H), 2.50−2.54 (m, 1H), 2.44 (s, 3H), 2.16 (d, J = 15 Hz, 1H), 1.58 (s, 3H), 1.41 (s, 3H).

1,1,1-Trifluoro-4-(5-fluoro-2-methyl-phenyl)-4-methyl-2-(2-pyrrolidin-1-yl-5*H*-pyrrolo[3,2-*d*]pyrimidin-6-ylmethyl)-pentan-2-ol (29). Following the general Sonogashira coupling procedure starting from **17a** and **25d** gave 2,2,2-trifluoro-*N*-{4-[6-(5-fluoro-2-methyl-phenyl)-4-hydroxy-6-methyl-4-trifluoromethyl-hept-1-ynyl]-2-pyrrolidin-1-yl-pyrimidin-5-yl}-acetamide (52% yield).

Following the general cyclization procedure B starting from 2,2,2-trifluoro-*N*-{4-[6-(5-fluoro-2-methyl-phenyl)-4-hydroxy-6-methyl-4-trifluoromethyl-hept-1-ynyl]-2-pyrrolidin-1-yl-pyrimidin-5-yl}-acetamide gave **29** as a (36% yield). ^{1}H NMR (400 MHz, DMSO-d_6) δ 10.54 (s, 1H), 8.40 (s, 1H), 7.08−7.13 (m, 2H), 6.89−6.92 (m, 1H), 6.04 (s, 1H), 5.96 (s, 1H), 3.44−3.47 (m, 4H), 2.79 (d, J = 15 Hz, 1H), 2.64 (d, J = 15 Hz, 1H), 2.41 (s, 3H), 2.38−2.41 (m, 1H), 2.15 (d, J = 16 Hz, 1H), 1.89−1.91 (m, 4H), 1.52 (s, 3H), 1.40 (s, 3H).

(*R*)-1,1,1-Trifluoro-4-(5-fluoro-2-methyl-phenyl)-4-methyl-2-(2-morpholin-4-yl-5*H*-pyrrolo[3,2-*d*]pyrimidin-6-ylmethyl)-pentan-2-ol (30). Following the general Sonogashira coupling procedure starting from **17a** and **25e** gave 2,2,2-trifluoro-*N*-{4-[(*S*)-6-(5-fluoro-2-methyl-phenyl)-4-hydroxy-6-methyl-4-trifluoromethyl-hept-1-ynyl]-2-morpholin-4-yl-pyrimidin-5-yl}-acetamide (46% yield).

Following the general cyclization procedure B starting from 2,2,2-trifluoro-*N*-{4-[(*S*)-6-(5-fluoro-2-methyl-phenyl)-4-hydroxy-6-methyl-4-trifluoromethyl-hept-1-ynyl]-2-morpholin-4-yl-pyrimidin-5-yl}-acetamide gave **30** as a (64% yield). ^{1}H NMR (400 MHz, DMSO-d_6) δ

dx.doi.org/10.1021/jm4019178 | *J. Med. Chem.* 2014, 57, 1583−1598

10.83 (s, 1H), 8.44 (s, 1H), 7.08−7.12 (m, 2H), 6.89 (td, J = 8 Hz, J = 3 Hz, 1H), 6.06 (s, 1H), 5.99 (s, 1H), 3.57−3.66 (m, 8H), 2.79 (d, J = 15 Hz, 1H), 2.62 (d, J = 15 Hz, 1H), 2.41 (d, J = 15 Hz, 1H), 2.41 (s, 3H), 2.13 (d, J = 15 Hz, 1H), 1.51 (s, 3H), 1.39 (s, 3H).

2-[2-(1,1-Dioxo-1λ6-thiomorpholin-4-yl)-5*H*-pyrrolo[3,2-*d*]-pyrimidin-6-ylmethyl]-1,1,1-trifluoro-4-(5-fluoro-2-methyl-phenyl)-4-methyl-pentan-2-ol (31). A solution of the alkyne **17a** (151 mg, 0.50 mmol), the chloro pyrimidine **25f** (90 mg, 0.25 mmol), and triethylamine (0.17 mL, 1.25 mmol) in CH_3CN (0.8 mL) was degassed by bubbling argon through for 5 min. $Pd(PPh_3)_2Cl_2$ (18 mg, 0.03 mmol) and CuI (4.7 mg, 0.03 mmol) were added. The reaction mixture was heated to 70 °C for 2 h. The reaction mixture was subjected to flash chromatography on silica gel using 0−100% EtOAc in CH_2Cl_2 to give **31** as an off-white solid (72% yield). ^{1}H NMR (400 MHz, DMSO-d_6) δ 11.01 (s, 1H), 8.55 (s, 1H), 7.16−7.20 (m, 2H), 6.97 (td, J = 8 Hz, J = 3 Hz, 1H), 6.18 (s, 1H), 6.10 (s, 1H), 4.25 (br s, 4H), 3.13 (br s, 4H) 2.86 (d, J = 15 Hz, 1H), 2.67 (d, J = 15 Hz, 1H), 2.54−2.56 (m, 1H), 2.49 (s, 3H), 2.20 (d, J = 15 Hz, 1H), 1.62 (s, 3H), 1.47 (s, 3H).

1,1,1-Trifluoro-4-(5-fluoro-2-methoxy-phenyl)-4-methyl-2-(5*H*-pyrrolo[3,2-*d*]pyrimidin-6-ylmethyl)-pentan-2-ol (32). Following the general Sonogashira coupling procedure starting from **17b**[16] and **8**[19] gave 1-(5-amino-pyrimidin-4-yl)-6-(5-fluoro-2-methoxy-phenyl)-6-methyl-4-trifluoromethyl-hept-1-yn-4-ol (57% yield).

Following the general cyclization procedure A starting from 1-(5-amino-pyrimidin-4-yl)-6-(5-fluoro-2-methoxy-phenyl)-6-methyl-4-trifluoromethyl-hept-1-yn-4-ol gave **32** as a white solid (63% yield). ^{1}H NMR (400 MHz, MeOH-d_4) δ 8.69 (s, 1H), 8.67 (s, 1H), 7.10 (d, J = 8 Hz, 1H), 6.90−6.92 (m, 2H), 6.27 (s, 1H), 3.83 (s, 3H), 3.10 (d, J = 15 Hz, 1H), 2.89 (d, J = 15 Hz, 1H), 2.63 (d, J = 15 Hz, 1H), 2.09 (d, J = 15 Hz, 1H), 1.63 (s, 3H), 1.40 (s, 3H).

1,1,1-Trifluoro-4-(2-methanesulfonyl-phenyl)-4-methyl-2-(5*H*-pyrrolo[3,2-*d*]pyrimidin-6-ylmethyl)-pentan-2-ol (34). Following the general Sonogashira coupling procedure starting from **17d** and **8**[19] gave 1-(5-amino-pyrimidin-4-yl)-6-(2-methanesulfonyl-phenyl)-6-methyl-4-trifluoromethyl-hept-1-yn-4-ol (53% yield).

Following the general cyclization procedure A starting from 1-(5-amino-pyrimidin-4-yl)-6-(2-methanesulfonyl-phenyl)-6-methyl-4-trifluoromethyl-hept-1-yn-4-ol gave **34** as a white foam (25% yield). ^{1}H NMR (400 MHz, DMSO-d_6) δ 11.35 (s, 1H), 8.75 (s, 1H), 8.70 (s, 1H), 8.17 (dd, J = 8 Hz, J = 1 Hz, 1H), 7.75 (d, J = 7 Hz, 1H), 7.62 (ddd, J = 8 Hz, J = 7 Hz, J = 1 Hz, 1H), 6.28 (s, 1H), 6.07 (s, 1H), 3.28 (s, 3H), 3.00 (d, J = 15 Hz, 1H), 2.87 (d, J = 16 Hz, 1H), 2.68 (d, J = 16 Hz, 1H), 2.43 (d, J = 15 Hz, 1H), 1.74 (s, 3H), 1.61 (s, 3H). ES-MS m/z = 442 $(M + H)^+$.

1,1,1-Trifluoro-4-(3-methanesulfonyl-phenyl)-4-methyl-2-(5*H*-pyrrolo[3,2-*d*]pyrimidin-6-ylmethyl)-pentan-2-ol (35). Following the general Sonogashira coupling procedure starting from **17e** and **8**[19] gave 1-(5-amino-pyrimidin-4-yl)-6-(3-methanesulfonyl-phenyl)-6-methyl-4-trifluoromethyl-hept-1-yn-4-ol (71% yield).

Following the general cyclization procedure A starting from 1-(5-amino-pyrimidin-4-yl)-6-(3-methanesulfonyl-phenyl)-6-methyl-4-trifluoromethyl-hept-1-yn-4-ol gave **35** as a white solid (30% yield). ^{1}H NMR (400 MHz, DMSO-d_6) δ 11.39 (s, 1H), 8.78 (s, 1H), 8.73 (s, 1H), 7.92 (s, 1H), 7.69−7.75 (m, 2H), 7.45−7.49 (m, 1H), 6.36 (s, 1H), 6.11 (s, 1H), 3.19 (s, 3H), 2.89 (d, J = 15 Hz, 1H), 2.89 (d, J = 14 Hz, 1H), 2.31 (d, J = 16 Hz, 1H), 2.23 (d, J = 15 Hz, 1H), 1.50 (s, 3H), 1.37(s, 3H). ES-MS m/z = 442 $(M + H)^+$.

1,1,1-Trifluoro-4-(5-fluoro-2,3-dihydro-benzofuran-7-yl)-4-methyl-2-(5*H*-pyrrolo[3,2-*d*]pyrimidin-6-ylmethyl)-pentan-2-ol (36). Following the general Sonogashira coupling procedure starting from **17f**[16] and **8**[19] gave 1-(5-amino-pyrimidin-4-yl)-6-(5-fluoro-2,3-dihydro-benzofuran-7-yl)-6-methyl-4-trifluoromethyl-hept-1-yn-4-ol (47% yield).

Following the general cyclization procedure A starting from 1-(5-amino-pyrimidin-4-yl)-6-(5-fluoro-2,3-dihydro-benzofuran-7-yl)-6-methyl-4-trifluoromethyl-hept-1-yn-4-ol gave **36** as a white solid (41% yield). ^{1}H NMR (400 MHz, MeOH-d_4) δ 8.60 (s, 1H), 8.58 (s, 1H), 6.71−6.75 (m, 2H), 6.21 (s, 1H), 4.45 (t, J = 9 Hz, 2H), 3.02 (t, J = 9 Hz, 2H), 2.86 (d, J = 16 Hz, 2H), 2.59 (d, J = 15 Hz, 1H), 2.59 (d, J = 15 Hz, 1H), 1.50 (s, 3H), 1.27 (s, 3H).

4-(5-Chloro-2,3-dihydro-benzofuran-7-yl)-1,1,1-trifluoro-4-methyl-2-(5*H*-pyrrolo[3,2-*d*]pyrimidin-6-ylmethyl)-pentan-2-ol (37). Following the general Sonogashira coupling procedure starting from **17g**[16] and **8**[19] gave 1-(5-amino-pyrimidin-4-yl)-6-(5-chloro-2,3-dihydro-benzofuran-7-yl)-6-methyl-4-trifluoromethyl-hept-1-yn-4-ol (24% yield).

Following the general cyclization procedure A starting from 1-(5-amino-pyrimidin-4-yl)-6-(5-chloro-2,3-dihydro-benzofuran-7-yl)-6-methyl-4-trifluoromethyl-hept-1-yn-4-ol gave **37** as a white solid (50% yield). ^{1}H NMR (400 MHz, MeOH-d_4) δ 8.70 (s, 1H), 8.68 (s, 1H), 7.04−7.05 (m, 2H), 6.32 (s, 1H), 4.55 (t, J = 8 Hz, 2H), 3.11 (t, J = 9 Hz, 2H), 2.93 (2d, J = 16 Hz, 2H), 2.71 (d, J = 15 Hz, 1H), 2.08 (d, J = 15 Hz, 1H), 1.59 (s, 3H), 1.36 (s, 3H). HPLC purity 94%.

1,1,1-Trifluoro-4-methyl-2-(5*H*-pyrrolo[3,2-*d*]pyrimidin-6-yl-methyl)-4-(2-methyl-phenyl)-pentan-2-ol (40). Step 1: A mixture 1,1,1-trifluoro-4-methyl-pent-3-en-2-one (800 mL, ∼0.45 M in THF, 0.35 mol) and CuI (33.3 g, 0.18 mol) was cooled to −20 °C. 2-Methylphenylmagnesum bromide (175 mL, 2 M in THF, 0.35 mol) was added, and the mixture was allowed to warm to room temperature and stirred for 2 h. The reaction was quenched with HCl (6 N in water, 500 mL) and filtered through Celite, and the layers were separated. The organic phase was dried over $MgSO_4$, filtered, and concentrated to give 1,1,1-trifluoro-4-methyl-4-(2-methylphenyl)-pentan-2-one as an oil (70% yield).

Step 2: To a solution of LHMDS (1 M in THF, 778 mL, 0.82 mol) at −65 °C was added methyl acetate (59 mL, 0.74 mol) over 15 min. 1,1,1-Trifluoro-4-methyl-4-(2-methylphenyl)-pentan-2-one (99 g, 0.41 mol) was added over 20 min. After 10 min, NaOH (4 M, 200 mL, 0.80 mol) was added and the mixture allowed to warm to room temperature. The reaction was stirred for 70 h at room temperature. The mixture was concentrated to remove THF, acidified with conc HCl to pH 1 and extracted with CH_2Cl_2 (1000 mL). The organic phase was separated, dried over $MgSO_4$, and concentrated. The residue was recrystallized from hexane to give 3-hydroxy-5-methyl-5-*o*-tolyl-3-trifluoromethyl-hexanoic acid as a white solid (53% yield).

Step 3: 3-Hydroxy-5-methyl-5-*o*-tolyl-3-trifluoromethyl-hexanoic acid (8.0 g, 17.6 mmol) in MeOH (40 mL) was treated with conc H_2SO_4 (2.0 mL) and heated to reflux for 16 h. The mixture was concentrated and then diluted with heptane and water. The organic layer was separated, and the aqueous layer was extracted with heptane (200 mL). The combined organic phases were washed with satd $NaHCO_3$ solution, dried over $MgSO_4$, and concentrated to give 3-hydroxy-5-methyl-5-*o*-tolyl-3-trifluoromethyl-hexanoic acid methyl ester as a yellow oil (100% yield).

Step 4: 3-Hydroxy-5-methyl-5-*o*-tolyl-3-trifluoromethyl-hexanoic acid methyl ester (66.0 g, 207 mmol) was dissolved in DMF (350 mL). At room temperature, imidazole (35.2 g, 518 mmol) was added, followed by TMSCl (39.7 mL, 311 mmol). After 20 h, NH_4Cl solution and Et_2O were added. The organic layer was separated, and the aqueous layer was extracted with Et_2O (200 mL). The combined organic phases were washed with satd brine, dried over $MgSO_4$, and concentrated to give 5-methyl-5-*o*-tolyl-3-trifluoromethyl-3-trimethyl-silanyloxy-hexanoic acid methyl ester as a colorless oil (95% yield).

Step 5: To a solution of 5-amino-4-methylpyrimidine (4.72 g, 43.3 mmol) in THF (210 mL) at −20 °C was added *n*-BuLi (2.5 M in hexane; 42.1 mL, 105 mmol). The reaction was allowed to warm to room temperature over 2.5 h. A solution of 5-methyl-5-*o*-tolyl-3-trifluoromethyl-3-trimethylsilanyloxy-hexanoic acid methyl ester (5.0 g, 13 mmol) in THF (5 mL) was added at room temperature. After 20 min, MeOH (42 mL) was added, followed by water (21 mL). After 18 h, HCl (6 N; 25 mL) was added and the mixture stirred for 2 h. The mixture was neutralized with NaOH (2 N) to pH 7. CH_2Cl_2 was added. The organic layer was separated, and the aqueous layer was extracted with CH_2Cl_2. The combined organic phases were dried over $MgSO_4$ and concentrated to give **40** as a tan foam (47% yield). ^{1}H NMR (400 MHz, DMSO-d_6) δ 11.31 (s, 1H), 8.75 (s, 1H), 8.70 (s, 1H), 7.40−7.38 (m, 1H), 7.14−7.06 (m, 3H), 6.27 (s, 1H), 6.17 (s,

dx.doi.org/10.1021/jm4019178 | J. Med. Chem. 2014, 57, 1583−1598

1H), 2.86−2.82 (m, 1H), 2.63−2.56 (m, 2H), 2.49 (s, 3H), 2.13−2.10 (m, 1H), 1.62 (s, 3H), 1.42 (s, 3H).

4-Fluoro-2-[4,4,4-trifluoro-3-hydroxy-1,1-dimethyl-3-(5*H*-pyrrolo[3,2-*d*]pyrimidin-6-ylmethyl)-butyl]-phenol (41). A solution of **32** (50 mg, 0.12 mmol) in CH_2Cl_2 (2 mL) at −15 °C was treated with a solution of BBr_3 (1 M in CH_2Cl_2, 1.2 mL, 1.2 mmol) in a dropwise fashion. The reaction mixture was stirred at 0 °C for 60 h. The reaction was quenched with satd aqueous $NaHCO_3$ solution until pH 7 was reached. The mixture was extracted with EtOAc (4 × 10 mL). The combined organic layers were dried over Na_2SO_4, filtered, and concentrated. The residue was purified by preparative TLC using 12% MeOH in CH_2Cl_2 to give **41** as a white solid (68% yield). ^{1}H NMR (400 MHz, MeOH-d_4) δ 8.71 (s, 1H), 8.67 (s, 1H), 7.03 (dd, J = 11 Hz, J = 2 Hz, 1H), 6.70−6.76 (m, 2H), 6.27 (s, 1H), 3.13 (d, J = 15 Hz, 1H), 2.96 (d, J = 15 Hz, 1H), 2.76 (d, J = 15 Hz, 1H), 2.12 (d, J = 15 Hz, 1H), 1.66 (s, 3H), 1.47 (s, 3H).

5-Fluoro-2-[4,4,4-trifluoro-3-hydroxy-1,1-dimethyl-3-(5*H*-pyrrolo[3,2-*d*]pyrimidin-6-ylmethyl)-butyl]-phenol (42). Following the general Sonogashira coupling procedure starting from **17c** and **8**[19] gave 1-(5-amino-pyrimidin-4-yl)-6-(4-fluoro-2-methoxy-phenyl)-6-methyl-4-trifluoromethyl-hept-1-yn-4-ol (70% yield).

Following the general cyclization procedure A starting from 1-(5-amino-pyrimidin-4-yl)-6-(4-fluoro-2-methoxy-phenyl)-6-methyl-4-trifluoromethyl-hept-1-yn-4-ol gave 1,1,1-trifluoro-4-(4-fluoro-2-methoxy-phenyl)-4-methyl-2-(5*H*-pyrrolo[3,2-*d*]pyrimidin-6-ylmethyl)-pentan-2-ol (**33**) as a solid (41% yield).

Step 3: **33** (110 mg, 0.27 mmol) was dissolved in CH_2Cl_2 (5 mL) and treated with BBr_3 (1 M in CH_2Cl_2, 2.5 mL, 2.5 mmol) at 0 °C. The mixture was allowed to stand at 4 °C for 18 h. The mixture was quenched by the dropwise addition of MeOH. The solvent was evaporated. EtOAc (10 mL) and water (10 mL) were added. Solid Na_2CO_3 was added until pH > 7. The organic phase was separated, and the aqueous layer was extracted with EtOAc (3 × 50 mL). The combined organic phases were dried over $MgSO_4$. The solvent was removed. The residue was purified by flash chromatography using 50−100% EtOAc in hexanes to yield **42** as a white solid (70% yield). ^{1}H NMR (400 MHz, MeOH-d_4) δ 8.59 (s 1H), 8.56 (s, 1H), 7.17 (dd, J = 9 Hz, J = 7 Hz, 1H), 6.38−6.42 (m, 2H), 6.15 (s, 1H), 3.14 (d, J = 15 Hz, 1H), 2.84 (d, J = 15 Hz, 1H), 2.55 (d, J = 15 Hz, 1H), 1.92 (d, J = 15 Hz, 1H), 1.56 (s, 3H), 1.34 (s, 3H). HPLC purity 92%.

GR, PR, and MR Binding Assays. GR, PR, and MR binding assays were performed in a fluorescence polarization microplate format that measures competition for binding to the nuclear receptor between a test compound and a fluorescently labeled receptor ligand or probe. The probes used for the assays were as follows. GR and MR assays, 5 nM tetramethylrhodamine-labeled dexamethasone; PR assay, 5 nM tetramethylrhodamine-labeled RU-486; for GR and MR assays, receptors present in lysates of baculovirus-infected insect cells coinfected with receptor, HSP-70, HSP-90, and p23 were used. For PR binding assays, lysates were generated from insect cells infected with receptor-containing baculovirus alone. Binding reactions consisted of lysate, test compound, and probe combined in assay buffer containing 10 mM TES, 50 mM KCl, 20 mM $Na_2MoO_4{\cdot}2H_2O$, 1.5 mM EDTA, 0.04% w/v CHAPS, 10% v/v glycerol, 1 mM dithiothreitol, pH = 7.4. Lysates containing GR, PR, and MR were diluted into the assay 300-fold, 13-fold, and 17-fold into the respective binding reactions. The DMSO concentration in all binding reactions was 1% (v/v). Following one hour incubation in the dark at room temperature, fluorescence polarization signal was measured using a Molecular Devices Analyst plate reader with excitation and emission filters of 550 and 580 nm selected and with a 561 nm dichroic mirror installed. Positive control FP signal was measured in assay wells containing binding reactions without inhibitor. The fluorescence polarization signal produced by maximal inhibition (background control) was determined using the signals from wells containing 2 μM concentrations of a standard inhibitor for each receptor: dexamethasone for GR and MR and RU-486 for PR. Fluorescence polarization signals from duplicate 11-point concentration−response curves were fitted to a four-parameter logistic equation to determine IC_{50} values.

IL-1 Induced IL-6 Assay (Transrepression). The fibroblast-IL-6 assay measures the ability of test compounds to inhibit the elaboration of IL-6 by human foreskin fibroblasts following stimulation by IL-1 in vitro. Human foreskin fibroblasts (ATCC no. CRL-2429) were grown in Iscove's media supplemented with 10% (v/v) charcoal/dextran-treated fetal bovine serum and plated at 20000 cells/well two days prior to assay. On the day of the assay, the media was replaced, followed by the addition of test compound (0.4% DMSO final assay concentration) and recombinant human IL-1 (final concentration = 1 ng/mL). After incubation at 37 °C for 18−24 h, IL-6 in the tissue culture media was quantitated using standard electrochemiluminescence, DELFIA, or ELISA methods. Test compound IC_{50} values were determined by fitting the data from duplicate 11-point concentration−response curves to a four-parameter logistic equation. In this assay, IL-6 inhibition is considered a measure of agonist response of the glucocorticoid receptor, and dexamethasone is considered to possess 100% efficacy.

MMTV Reporter Gene Assay (Transactivation). HeLa MMTV transactivation assay measures the ability of test compounds to activate MMTV promoter in HeLa cells stably transfected with MMTV luciferase construct. HeLa MMTV cells were grown in DMEM media supplemented with 10% (v/v) fetal bovine serum (Hyclone), 100 U/mL penicillin, 100 μg/mL streptomycin, 2 mM L-glutamine, and 300 μg/mL genetecin. The day prior to assay the cells were plated at 25000 cells/well in 96-well white clear-bottom cell culture plates in DMEM media supplemented with 3% (v/v) FBS, 100 U/mL penicillin, 100 μg/mL streptomycin, and 2 mM L-glutamine. On the day of the assay, the media was replaced, followed by addition of test compound (0.2% DMSO final assay concentration). Positive control wells received 1 μM dexamethasone and represent 100% induction, while negative control wells received vehicle only and represent background. After final addition of the compounds, plates were incubated for 6 h at 37 °C and 5% CO_2. After incubation period, luminescence was detected upon cell lysis with Steady Glow Luciferase Reagent (Promega no. E2520). Activation of MMTV promoter by test compounds is expressed in percentage relative to positive control. Test compound EC_{50} values were determined by nonlinear curve fitting of the data from duplicate eight-point concentration−response curve.

Osteocalcin Production Assay. Osteocalcin is a marker of bone formation in bone growth and remodeling. It is produced by osteoblasts and is the most abundant noncollagenous bone matrix protein. Human MG-63 cells, an osteosarcoma cell line of osteoblast lineage, produce osteocalcin upon stimulation with vitamin D. The addition of dexamethasone effectively inhibits the vitamin D-induced osteocalcin production in MG-63. Compounds that bind to the glucocorticoid receptor and inhibit IL-1-induced IL-6 expression in human foreskin fibroblast cells were evaluated for their ability to inhibit osteocalcin production in MG-63 cells.

Human osteosarcoma MG-63 cells (ATCC) were plated on 96-well plates at 20000 cells per well on day 1 in 200 μL of media of 99% DMEM/F-12 (Gibco-Invitrogen), supplemented with 1% penicillin and streptomycin (Gibco-Invitrogen), 10 μg/mL vitamin C (Sigma), and 1% charcoal filtered fetal bovine serum (HyClone). On day 2, wells were replaced with fresh media. Cells were treated with vitamin D (Sigma) to a final concentration of 10 nM and with the test compounds in concentrations of 2×10^{-6} M to 10^{-10} M in a total volume of 200 μL per well. Samples were tested in duplicates. Background control wells did not receive vitamin D or compounds. Positive control wells received vitamin D only, without compounds, and represented maximum (100%) amount of osteocalcin production. Plates were incubated at 37 °C incubator for 48 h, and supernatants were harvested at the end of incubation. Amounts of osteocalcin in the supernatants were determined by the Gla-type osteocalcin ELISA kit (Zymed) according to manufacturer's protocol. Inhibition of osteocalcin by test compounds is expressed in percentage relative to positive controls. IC_{50} values of the test compounds were derived by nonlinear curve fitting.

In Vivo LPS-Challenge Assay. Female Balb/c mice, weighing approximately 20 g, were administered the test compound in cremophor (po) approximately 60 min prior to LPS/D-gal

administration. The volume of oral gavage was 0.15 mL. Then mice were administered LPS (*Escherichia coli* LPS 055:85, 1.0 μg/mouse) plus D-gal (50 mg/kg) intravenously in 0.2 mL of pyrogen-free saline. One hour after LPS/D-gal, each mouse was anesthetized, bled by cardiac puncture, and collected for serum TNF-α and compound levels. Blood samples were centrifuged at 2500 rpm for 10−15 min, the serum was decanted, and samples were stored frozen at −70 °C until transfer either for TNF-α determination or for plasma concentration analysis by HPLC. The concentration of TNF-α in the serum was measured by a commercially available ELISA kit (R&D Systems, Minneapolis, MN). ELISA was performed according to the manufacturers assay procedure. All samples are assayed in duplicate.

Collagen Induced Arthritis. Female B10.RIII mice (Jackson Laboratories) were immunized intradermally at 12−15 weeks of age with lyophilized native porcine type II collagen (CII lot P9603, purchased from Dr. Marie Griffiths, Utah University) dissolved overnight at 4 °C in 0.01 N acetic acid at a concentration of 2 mg/mL. The collagen solution was then emulsified at a 1:1 ratio with complete Freund's adjuvant (containing 2 mg/mL *Mycobacterium tuberculosis* strain H37Ra). On day 0, animals received a single intradermal injection of 100 μL (containing 100 μg type II collagen) of cold emulsion in the base of the tail. Beginning on day 13 post immunization, all immunized animals were monitored daily for signs of clinical arthritis. Arthritic animals were randomly enrolled into treatment groups until a total of 10 animals per group was achieved. Upon enrollment, the animal was anesthetized with 50 mg/kg (10 mg/mL) ketamine/15 mg/kg (2 mg/mL) zylazine. A whole body noninvasive density scan was performed to assess body fat content. (PIXImus densitometer, Lunar Corp.). Three to four h after recovering from anesthesia, the animal received the appropriate treatment once a day for a period of 35 days. Disease progression and severity were assessed every Monday, Wednesday, and Friday for 5 weeks. A clinical scoring system was used whereby each limb was graded as follows: 0, normal; 1, erythema and edema in 1−2 digits; 2, erythema and edema in >2 digits or severe edema and erythema encompassing the tarsal and metatarsal joints; 3, edema and erythema encompassing the tarsal and metatarsal joints along with joint deformity. At termination (day 35), a serum sample was collected for biomarker analysis. Triglyceride levels were determined with the Wako L-Type TG-H kit (Wako Diagnostics, Richmond, VA). Free fatty acids in serum were measured using the Wako NEFA-C microtiter procedure (Wako Diagnostics, Richmond, VA, catalogue no. 994−75409). For the serum insulin assay, the Ultra Sensitive Rat Insulin ELISA Kit (Crystal Chem Inc., Chicago, IL, catalogue no. 90060) and Mouse Insulin Standard 1.28 ng (catalogue no. 90090) was used.

AUTHOR INFORMATION

Corresponding Author

*Phone: (203) 778 7924. Fax: (203) 791 6072. E-mail: christian.harcken@boehringer-ingelheim.com.

Notes

The authors declare no competing financial interest.

ABBREVIATIONS USED

AP-1, activator protein 1; CHAPS, 3-[(3-cholamidopropyl)-dimethylammonio]-1-propanesulfonate; CIA, collagen induced arthritis; DMEM, Dulbecco's Modified Eagle Medium; FBS, fetal bovine serum; GC, glucocorticoid; GR, glucocorticoid receptor; GRE, glucocorticoid response element; IL-1, interleukin 1; MMTV, mouse mammary tumor virus; MR, mineralocorticoid receptor; PR, progesterone receptor; Qh, hepatic blood flow; RA, rheumatoid arthritis; TA, transactivation; TR, transrepression

REFERENCES

(1) (a) Gupta, R.; Jindal, D. P.; Kumar, G. Corticosteroids: the mainstay in asthma therapy. *Bioorg. Med. Chem.* **2004**, *12*, 6331−6342. (b) Buttgereit, F.; Saag, K. G.; Cutolo, M.; da Silva, J. A. P.; Bijlsma, J. W. J. The molecular basis for the effectiveness, toxicity, and resistance to glucocorticoids: focus on the treatment of rheumatoid arthritis. *Scand. J. Rheumatol.* **2005**, *34*, 14−21.

(2) Schäcke, H.; Döcke, W.-D.; Asadullah, K. Mechanisms involved in the side effects of glucocorticoids. *Pharmacol. Ther.* **2002**, *96*, 23−43.

(3) (a) Kanis, J. A.; Stevenson, M.; McCloskey, E. V.; Davis, S.; Lloyd-Jones, M. Glucocorticoid-induced osteoporosis: a systematic review and cost-utility analysis. *Health Technol. Assess.* **2007**, *11*, iii−89. (b) Hofbauer, L. C.; Rauner, M. Minireview: Live and let die: Molecular effects of glucocorticoids on bone cells. *Mol. Endocrinol.* **2009**, *23*, 1525−1531. (c) Weinstein, R. S. Glucocorticoid-induced bone disease. *N. Engl. J. Med.* **2011**, *365*, 62−70.

(4) (a) Zhou, J.; Cidlowski, J. A. The human glucocorticoid receptor: one gene, multiple proteins and diverse responses. *Steroids* **2005**, *70*, 407−417. (b) Adcock, I. M. Molecular mechanisms of glucocorticosteroid actions. *Pulm. Pharmacol. Ther.* **2000**, *13*, 115−126.

(5) Grad, I.; Picard, D. The glucocorticoid responses are shaped by molecular chaperones. *Mol. Cell. Endocrinol.* **2007**, *275*, 2−12.

(6) Clark, A. R.; Belvisi, M. G. Maps and legends: the quest for dissociated ligands of the glucocorticoid receptor. *Pharmacol. Ther.* **2012**, *134*, 54−67.

(7) (a) Schäcke, H.; Rehwinkel, H.; Asadullah, K. Dissociated glucocorticoid receptor ligands: compounds with an improved therapeutic index. *Curr. Opin. Invest. Drugs* **2005**, *6*, 503−507. (b) Newton, R.; Holden, N. S. Separating transrepression and transactivation: a distressing divorce for the glucocorticoid receptor? *Mol. Pharmacol.* **2007**, *72*, 799−809. (c) De Bosscher, K.; Haegeman, G.; Elewaut, D. Targeting inflammation using selective glucocorticoid receptor modulators. *Curr. Opin. Pharmacol.* **2010**, *10*, 497−504. (d) Glass, C. K.; Saijo, K. Nuclear receptor transrepression pathways that regulate inflammation in macrophages and T cells. *Nature Rev. Immunol.* **2010**, *10*, 365−376.

(8) (a) Reichardt, H. M.; Kaestner, K. H.; Tuckermann, J.; Kretz, O.; Wessely, O.; Bock, R.; Gass, P.; Schmid, W.; Herrlich, P.; Angel, P.; Schütz, G. DNA binding of the glucocorticoid receptor is not essential for survival. *Cell* **1998**, *93*, 531−541. (b) Cole, T. J.; Blendy, J. A.; Monaghan, A. P.; Krieglstein, K.; Schmid, W.; Aguzzi, A.; Fantuzzi, G.; Hummler, E.; Unsicker, K.; Schütz, G. Targeted disruption of the glucocorticoid receptor gene blocks adrenergic chromaffin cell development and severely retards lung maturation. *Genes Dev.* **1995**, *9*, 1608−1621. (c) Tuckermann, J. P.; Reichardt, H. M.; Arribas, R.; Richter, K. H.; Schütz, G.; Angel, P. The DNA binding-independent function of the glucocorticoid receptor mediates repression of AP-1-dependent genes in skin. *J. Cell Biol.* **1999**, *147*, 1365−1370. (d) Reichardt, H. M.; Tuckermann, J. P.; Gottlicher, M.; Vujic, M.; Weih, F.; Angel, P.; Herrlich, P.; Schütz, G. Repression of inflammatory responses in the absence of DNA binding by the glucocorticoid receptor. *EMBO J.* **2001**, *20*, 7168−7173.

(9) Rao, N. A. S.; McCalman, M. T.; Moulos, P.; Francoijs, K.-J.; Chatziioannou, A.; Kolisis, F. N.; Alexis, M. N.; Mitsiou, D. J.; Stunnenberg, H. G. Coactivation of GR and NFKB alters the repertoire of their binding sites and target genes. *Genome Res.* **2011**, *21*, 1404−1416.

(10) (a) Resche-Rigon, M.; Gronemeyer, H. Therapeutic potential of selective modulators of nuclear receptor action. *Curr. Opin. Chem. Biol.* **1998**, *2*, 501−507. (b) Barnes, P. J. Anti-inflammatory actions of glucocorticoids: molecular mechanisms. *Clin. Sci.* **1998**, *94*, 557−572. (c) Buckbinder, L.; Robinson, R. P. The Glucocorticoid Receptor: Molecular Mechanism and New Therapeutic Opportunities. *Curr. Drug Targets: Inflammation Allergy* **2002**, *1*, 127−136. (d) Burnstein, K. L.; Cidlowski, J. A. The down side of glucocorticoid receptor regulation. *Mol. Cell. Endocrinol.* **1992**, *83*, C1−C8.

(11) (a) Razavi, H.; Harcken, C. Non-steroidal Dissociated Glucocorticoid Receptor Agonists. *In Anti-Inflammatory Drug Discov-*

ery; Levin, J.; Laufer, S., Eds.; RSC Publishing: London, 2012; pp 481−516. (b) Berlin, M. Recent Advances in the Advancement of Glucocorticoid Receptor Modulators. *Expert Opin. Ther. Patents* **2010**, *20*, 855−873. (c) DeBosscher, K. Selective Glucocorticoid Modulators. *J. Steroid Biochem. Mol. Biol.* **2010**, *120*, 96−104.

(12) Marshall, D.; Rodriguez, G.; Thomson, D. S.; Nelson, R.; Capolina, A. α-Methyltryptamine sulfonamide derivatives as novel glucocorticoid receptor ligands. *Bioorg. Med. Chem. Lett.* **2007**, *17*, 315−319.

(13) Regan, J.; Lee, T. W.; Zindell, R. M.; Bekkali, Y.; Bentzien, J.; Gilmore, T.; Hammach, A.; Kirrane, T. M.; Kukulka, A. J.; Kuzmich, D.; Nelson, R. M.; Proudfoot, J. R.; Ralph, M.; Pelletier, J.; Souza, D.; Zuvela-Jelaska, L.; Nabozny, G.; Thomson, D. S. Quinol-4-ones as steroid A-ring mimetics in nonsteroidal dissociated glucocorticoid agonists. *J. Med. Chem.* **2006**, *49*, 7887−7896.

(14) Takahashi, H.; Bekkali, Y.; Capolino, A. J.; Gilmore, T.; Goldrick, S. E.; Kaplita, P. V.; Liu, L.; Nelson, R. M.; Terenzio, D.; Wang, J.; Zuvela-Jelaska, L.; Proudfoot, J.; Nabozny, G.; Thomson, D. Discovery and SAR study of novel dihydroquinoline containing glucocorticoid receptor agonists. *Bioorg. Med. Chem. Lett.* **2007**, *17*, 5091−5095.

(15) Kuzmich, D.; Kirrane, T.; Proudfoot, J.; Bekkali, Y.; Zindell, R.; Beck, L.; Nelson, R.; Shih, C.-K.; Kukulka, A. J.; Paw, Z.; Reilly, P.; Deleon, R.; Cardozo, M.; Nabozny, G.; Thomson, D. Identification of dissociated non-steroidal glucocorticoid receptor agonists. *Bioorg. Med. Chem. Lett.* **2007**, *17*, 5025−5031.

(16) Riether, D.; Harcken, C.; Razavi, H.; Kuzmich, D.; Gilmore, T.; Bentzien, J.; Pack, E. J., Jr.; Souza, D.; Nelson, R. M.; Kukulka, A.; Fadra, T. N.; Zuvela-Jelaska, L.; Pelletier, J.; Dinallo, R.; Panzenbeck, M.; Torcellini, C.; Nabozny, G. H.; Thomson, D. S. Non-steroidal Dissociated Glucocorticoid Agonists Containing Azaindoles as Steroid A-Ring Mimetics. *J. Med. Chem.* **2010**, *53*, 6681−6698.

(17) Betageri, R.; Gilmore, T.; Kuzmich, D.; Kirrane, T. M.; Bentzien, J.; Wiedenmeyer, D.; Regan, J.; Kukulka, A. J.; Fadra, T. N.; Nelson, R. M.; Zuvela-Jelaska, L.; Souza, D.; Pelletier, J.; Proudfoot, J.; Dinallo, R.; Panzenbeck, M.; Torcellini, C.; Lee, H.; Pack, E.; Harcken, C.; Nabozny, G.; Thomson, D. S. Non-steroidal Dissociated Glucocorticoid Agonists: lndoles as A-Ring Mimetics and Function-Regulating Pharmacophores. *Bioorg. Med. Chem. Lett.* **2011**, *21*, 6842−6851.

(18) Harcken, C.; Ward, Y.; Thomson, D.; Riether, D. A general and efficient synthesis of azaindoles and diazaindoles. *Synlett* **2005**, *20*, 3121−3125.

(19) Bekkali, Y.; Betageri, R.; Emmanuel, M. J.; Hammach, A.; Harcken, C. H. J. J.; Kirrane, T. M.; Kuzmich, D.; Lee, T., W.-H.; Liu, P.; Patel, U. R.; Razavi, H.; Riether, D. 1,1,1-Trifluoro-4-phenyl-4-methyl-2-(1*H*-pyrrolo[2,3-*c*]pyridine-2-ylmethyl)-pentan-2-ol derivatives and related compounds as glucocorticoid ligands for the treatment of inflammatory diseases and diabetes. Patent WO2005/030213, 2005.

(20) Bourotte, M.; Pellegrini, N.; Scmitt, M.; Bourguignon, J.-J. Expeditive Synthesis of 4-Substituted 3-Aminopyridazines. *Synlett* **2003**, 1482−1484.

(21) Dennin, F.; Blondeau, D.; Sliwa, H. Synthesis of derivatives of pyrazino[1,2-*a*]pyrimidin-4-ones. *J. Heterocycl. Chem.* **1990**, *27*, 1639−1643.

(22) Lee, T. W.; Proudfoot, J. R.; Thomson, D. S. A concise asymmetric route for the synthesis of a novel class of glucocorticoid mimetics containing a trifluoromethyl-substituted alcohol. *Bioorg. Med. Chem. Lett.* **2006**, *16*, 654−657.

(23) Bledsoe, R. K.; Montana, V. G.; Stanley, T. B.; Delves, C. J.; Apolito, C. J.; McKee, D. D.; Consler, T. G.; Parks, D. J.; Stewart, E. L.; Willson, T. M.; Lambert, M. H.; Moore, J. T.; Pearce, K. H.; Xu, H. E. Crystal Structure of the Glucocorticoid Receptor Ligand Binding Domain Reveals a Novel Mode of Receptor Dimerization and Coactivator Recognition. *Cell* **2002**, *110*, 93−105.

(24) Waage, A.; Slupphaug, G.; Shalaby, R. Glucocorticoids inhibit the production of IL6 from monocytes, endothelial cells and fibroblasts. *Eur. J. Immunol.* **1990**, *20*, 2439−2443.

(25) Suino-Powell, K.; Xu, Y.; Zhang, C.; Tao, Y.-g.; Tolbert, W. D.; Simons, S. S., Jr.; Xu, H. E. Doubling the Size of the Glucocorticoid Receptor Ligand Binding Pocket by Deacylcortivazol. *Mol. Cell. Biol.* **2008**, *28*, 1915−1923.